



1 **Emission characteristics of reactive organic gases from**
2 **industrial volatile chemical products (VCPs) in China**

3 **Sihang Wang^{1,2}, Bin Yuan^{1,2,*}, Xianjun He^{1,2}, Ru Cui^{1,2,a}, Xin Song^{1,2}, Yubin Chen^{1,2},**
4 **Caihong Wu^{1,2}, Chaomin Wang^{1,2}, Yibo Huangfu^{1,2}, Xiaobing Li^{1,2}, Boguang**
5 **Wang^{1,2}, Min Shao^{1,2}**

6 ¹ Institute for Environmental and Climate Research, Jinan University, Guangzhou
7 511443, China

8 ² Guangdong-Hongkong-Macau Joint Laboratory of Collaborative Innovation for
9 Environmental Quality, Guangzhou 511443, China

10 ^a now at: Nanjing Intelligent Environmental Science and Technology Co.Ltd, Nanjing
11 211800, China

12

13 *Email: byuan@jnu.edu.cn

14

15



16 **Abstract:**

17 Volatile chemical products (VCPs) have become an important source of reactive
18 organic gases (ROGs) in urban areas worldwide. Industrial activities can also utilize a
19 large amount of VCPs and emit many organic gases into the atmosphere. Due to
20 multiple sampling and measurement challenges, only a subset of ROG species is usually
21 measured for many industrial VCP sources. This study aimed to investigate the
22 emissions of ROGs from five industrial VCP sources in China, including shoemaking,
23 plastic surface coating, furniture coating, printing, and ship coating industries. More
24 comprehensive speciation of ROG emissions from these industrial VCP sources was
25 developed by the combination of the proton transfer reaction time-of-flight mass
26 spectrometer (PTR-ToF-MS) along with gas chromatography-mass spectrometer/flame
27 ionization detector (GC-MS/FID). Our study identified oxygenated ROG species
28 (OVOCs) as representative ROGs emitted from these sources, which are highly related
29 to specific chemicals used during the industrial activities. Moreover, mass spectra
30 similarity analysis revealed significant dissimilarities among the ROG emission sources,
31 indicating substantial variations between different industrial VCP sources. Except for
32 the ship coating industry utilizing solvent-borne coatings, the proportions of OVOCs
33 range from 67% to 96% in total ROG emissions and 72% to 97% in total OH reactivity
34 (OHR) for different industrial sources. The industrial VCP sources associated with
35 solvent-borne coatings exhibited a higher ozone formation potential (OFP), reaching as
36 high as 5.5 and 2.7 g O₃·g⁻¹ ROGs for ship coating and furniture coating industries,
37 primarily due to contributions from aromatics. The fractions of the ten most abundant
38 species in total ROG emissions, OHR, and OFP indicated a highly centralized of ROG
39 emissions from various industrial VCP sources. Our results suggest that ROG treatment
40 devices may have limited effectiveness for all ROGs, with treatment efficiencies
41 ranging from -12% to 68%. Furthermore, we found that ROG pairs (e.g., methyl ethyl
42 ketone (MEK) /C₈ aromatics ratio) could serve as effective indicators for distinguishing
43 industrial VCP sources, particularly for measurements in industrial areas. Our study
44 demonstrated the importance of measuring a large number of ROGs using PTR-ToF-



45 MS for characterizing ROG emissions from industrial VCP sources.

46



47 **1. Introduction**

48 With the successful control of vehicular emissions, emission from volatile
49 chemical products (VCPs) have become an increasingly significant source in cities all
50 around the world (Sun et al., 2018;McDonald et al., 2018;Li et al., 2019;Khare and
51 Gentner, 2018;Seltzer et al., 2022;Sasidharan et al., 2023). Reactive organic gases
52 (ROGs), organic gases other than methane, from VCPs emission can contribute
53 substantially to both anthropogenic secondary organic aerosol (SOA) and ozone (O₃)
54 in urban environments (Seltzer et al., 2022;Khare et al., 2022;Sasidharan et al.,
55 2023;Coggon et al., 2021;Gkatzelis et al., 2021b;Qin et al., 2021). With the
56 development of economy and industrialization, the emissions of industrial VCPs
57 contribute to approximately 25%-45% of ROG emissions in China (Ou et al., 2015;Wei
58 et al., 2011;Huang et al., 2011;Sha et al., 2021;Zhou et al., 2020b). To effectively
59 control atmospheric pollution in urban areas and surrounding regions, it becomes
60 imperative to gain a comprehensive understanding of the emission characteristics of
61 ROGs from industrial VCP sources.

62 Extensive research has been conducted to investigate ROG emissions from
63 industrial VCP sources, mainly focusing on sampling within manufacturing workshops
64 and exhaust stacks (Zheng et al., 2013;Yuan et al., 2010;Wang et al., 2014). Previous
65 studies have demonstrated that the use of individual chemicals (i.e. coatings, inks, and
66 adhesives) significantly impact on ROG emissions (Gkatzelis et al., 2021a;Zheng et al.,
67 2013;He et al., 2022a), and these chemicals used for printing, furniture, and shoemaking
68 industries has seen rapid growth and widespread adoption in recent years (Gkatzelis et
69 al., 2021a;McDonald et al., 2018;Seltzer et al., 2022;Coggon et al., 2021). Consequently,
70 the diverse emission sources and emission factors from industrial VCP sources have
71 contributed to large uncertainties (Mo et al., 2021;Zhong et al., 2018). To mitigate the
72 emissions of most primary pollutants, stricter emission standards have been
73 implemented along with advancements in ROG treatment technologies. Specifically,
74 water-borne VCPs has substituted solvent-borne VCPs in China (Mo et al., 2021;Li et
75 al., 2019;Shi et al., 2023). As a result, the emission characteristics of ROGs from



76 industrial VCP sources may undergo changes in response to the ongoing development
77 of VCPs and ROG treatment technologies. It is imperative to regularly updated the
78 understanding of ROG emission characteristics associated with industrial VCP sources.

79 The emissions of oxygenated ROG species (OVOCs) have been identified as
80 significant components in industrial VCP emissions (Chang et al., 2022; Mo et al.,
81 2021; Sha et al., 2021). For instance, it has been found that more than 80% of total ROG
82 emissions for shoemaking and printing industries are attributed to OVOC emissions
83 (Zheng et al., 2013). This notable contributions of OVOCs, such as acetone, methyl
84 ethyl ketone (MEK), ethyl acetate, and isopropanol, can be primarily attributed to the
85 use of individual industrial chemicals (Zheng et al., 2013; Wu et al., 2020b).
86 Traditionally, the collection of ROGs involved the use of canisters or Tedlar bags, and
87 their analysis was conducted using gas chromatography-mass spectrometer/flame
88 ionization detector (GC-MS/FID) techniques, with a primary focus on hydrocarbon
89 emissions (Yuan et al., 2010; Wang et al., 2014). Previous studies commonly employed
90 2,4-dinitrophenylhydrazine (DNPH) cartridges for collection and analyzed them using
91 high-performance liquid chromatography (HPLC) to detect carbonyl species such as
92 aldehydes and ketones. However, this approach is both time-consuming and susceptible
93 to contaminations (Mo et al., 2016; Han et al., 2019).

94 Due to the intricate chemical compositions of industrial VCPs, it is essential to
95 characterize ROG emissions with higher mass resolution. The proton-transfer-reaction
96 time-of-flight mass spectrometer (PTR-ToF-MS) has been extensively utilized for the
97 identification of VCP sources. It has been confirmed that VCP sources is a significant
98 contributor to ROG emissions. For instance, ROG emissions from VCP contribute 50%-
99 80% of anthropogenic ROG emissions in US cities (Gkatzelis et al., 2021b; McDonald
100 et al., 2018). The large fractions (~50%) of ROGs have been attributed to VCP-
101 dominated source in Guangzhou, highlighting its importance in urban environments (Li
102 et al., 2022). Through high mass resolution analysis, tracer compounds for various VCP
103 categories have been identified (Gkatzelis et al., 2021a; Coggon et al., 2018; Stockwell
104 et al., 2021). In addition, OVOCs such as acetates, acrylates, alcohols (e.g. benzyl



105 alcohol), glycols (e.g. propylene glycol, ethylene glycol), and glycol ethers, have been
106 found to make significant contributions to VCPs emission (Seltzer et al., 2021; Li and
107 Cocker, 2018; Li et al., 2018; Khare et al., 2022). With the ability to measure whole mass
108 spectra and offer high mass resolution, the PTR-ToF-MS enables more comprehensive
109 detection of a wide range of ROGs (Cappellin et al., 2012; Yuan et al., 2017; Huangfu et
110 al., 2021). By employing parameterization methods to determine instrument sensitivity,
111 more ROGs can be quantified from the obtained mass spectra (Sekimoto et al., 2017; Wu
112 et al., 2020a). Furthermore, previous studies have demonstrated that higher alkanes,
113 including acyclic, cyclic and bicyclic alkanes can be measured using PTR-ToF-MS with
114 NO^+ chemical ionization (NO^+ PTR-ToF-MS) (Inomata et al., 2014; Koss et al.,
115 2016; Wang et al., 2020; Chen et al., 2022). Higher alkanes are significant species in
116 vehicle and combustion emissions (Gao et al., 2023; Liu et al., 2021; Zhao et al., 2018b),
117 and they were not included in previous measurements of industrial VCP sources. Thus,
118 by combining hydrocarbons measured by offline GC-MS/FID, PTR-ToF-MS shows
119 promise as a method for developing more comprehensive speciation relevant to
120 industrial VCP emissions (Gao et al., 2023).

121 In this study, we applied a PTR-ToF-MS employing H_3O^+ and NO^+ chemical
122 ionization along with a GC-MS/FID to comprehensively measure ROG emissions from
123 five industrial VCP sources, including shoemaking, plastic surface coating, furniture
124 coating, printing, and ship coating industries in the Pearl River Delta (PRD) region of
125 China. We investigated emission characteristics of ROGs from semi-open workshops
126 and ROG treatment devices across these industries. We utilized the dataset to analyze
127 the contributions of different ROG components to total ROG emissions, OH reactivity
128 (OHR), ozone formation potential (OFP), and volatility in various industrial VCP
129 sources. Furthermore, we conducted intercomparisons of the mass spectra
130 characterizations of ROG emissions, which revealed significant variations in ROG
131 emissions from industrial VCP sources.

132 **2. Materials and methods**

133 **2.1 Tested industrial VCP sources and sampling methods**



134 Based on comprehensive analysis of written data, consultation with relevant
135 experts, and thorough on-site investigations, we selected five representative factories
136 and industries from various industrial VCP sources. The selection criteria for these
137 industries were based on relevant emission inventory research conducted in the PRD
138 region of China (Zhong et al., 2018). Sampling methods focused on capturing ROG
139 emissions generated during the main manufacturing processes, such as coatings
140 spraying and adhesives usage in the factories. Both online measurements and offline
141 sampling were carried out in semi-open workshops, as well as ROG treatment devices
142 (i.e. before and after emission treatment, generally located at the front and rear sampling
143 ports of the ROG treatment devices) in the factories (Table. S1).

144 During the campaign, a mobile monitoring vehicle was equipped with online
145 measurement equipment and strategically parked near the sampling ports of both
146 workshops and ROG treatment devices emissions (Fig. S1). A CO₂/H₂O gas analyzer
147 (LI-COR 840A, Inc., USA) was used to measure the concentrations of CO₂ and H₂O.
148 To ensure continuous sampling, air from various factories was drawn through a length
149 of Perfluoroalkoxy (PFA) Teflon tubing, ranging from 10 to 100 meters, at a controlled
150 flow rate of 6 L/min facilitated by an external pump.

151 **2.2 ROG measurements**

152 In this study, ROG were measured using a proton transfer reaction quadrupole
153 interface time-of-flight mass spectrometer (PTR-QiToF-MS) (IONICON Analytik,
154 Innsbruck, Austria) (Sulzer et al., 2014) and a combination of canister sampling and
155 offline GC-MS/FID analysis system (canister-GC-MS/FID). More comprehensive
156 speciation of ROG was achieved by analyzing hydrocarbons by canister-GC-MS/FID,
157 quantifying all signals using H₃O⁺ PTR-ToF-MS, and supplementing by acyclic, cyclic,
158 and bicyclic alkanes from NO⁺ ionization of PTR-ToF-MS. The selection of
159 overlapping ROGs was similar to a previous study (Gao et al., 2023).

160 To capture the real-time emission characteristics of ROGs from industrial VCP
161 sources, the mass spectra of PTR-ToF-MS was recorded every 10 s. Prior to each test,
162 background measurements of the instrument were carried out by passing sampling air



163 through a custom-built platinum catalytical converter that had been preheated to 365 °C
164 for 1 minute. Throughout the campaign, the PTR-ToF-MS instrument automatically
165 alternated between two reagent ions (H_3O^+ and NO^+) every 10 minutes. Detailed setting
166 parameters for H_3O^+ and NO^+ chemical modes in this instrument can be found in
167 previous studies (Wu et al., 2020a; Wang et al., 2020; He et al., 2022b). The Tofware
168 software package (version 3.0.3, ToFwerk AG, Switzerland) was employed to facilitate
169 accurate data analysis (Stark et al., 2015).

170 Calibration for ROGs measure by PTR-ToF-MS were carried out both in the
171 laboratory and during the campaign. The PTR-ToF-MS was regularly calibrated using
172 a 23-component gas standard (Linde Spectra) throughout the campaign. During the later
173 period of the campaign, two gas standards (Apel Riemer Environmental Inc.) were used
174 for the calibration of other ROGs, specifically for acyclic and cyclic alkanes using NO^+
175 chemical ionization. (Wang et al., 2020; Chen et al., 2022; Wang et al., 2022). A total of
176 11 organic acids and nitrogen-containing compounds were calibrated using the liquid
177 calibration unit (LCU, IONICON Analytik, Innsbruck, Austria) (Table. S2-S4). In order
178 to account for the humidity dependence of some ROGs in the PTR-ToF-MS (Yuan et
179 al., 2017; Koss et al., 2018), humidity-dependence curves established in the laboratory
180 were utilized for correction (Wu et al., 2020a; He et al., 2022b; Wang et al., 2022).
181 Sensitivities of uncalibrated species were determined based on the kinetics of proton-
182 transfer reactions of H_3O^+ with ROGs (Fig. S2) (Cappellin et al., 2012; Sekimoto et al.,
183 2017), with an associated uncertainty of approximately 50% for the concentrations of
184 uncalibrated species.

185 Simultaneously, offline sampling was conducted near the sampling ports of
186 workshops and ROG treatment devices. Whole air samples were collected using
187 canisters for determination of hydrocarbons in industrial VCP sources, and analyzed by
188 an offline GC-MS/FID system.. The GC-MS/FID system was calibrated using
189 photochemical assessment monitoring stations (PAMS) and TO-15 standard mixtures,
190 which enabled the identification and quantification of a total of 94 hydrocarbons. More
191 information about this instrument and dataset for canister sampling and offline GC-



192 MS/FID system can be found elsewhere (Li et al., 2020).

193 **2.3 Calibrations of esters and isopropanol based on H₃O⁺ and NO⁺** 194 **ionization**

195 Since ester species (including acetates and acrylates) play a significant role in
196 industrial VCP sources, it is important to accurately quantify their concentrations
197 (Khare et al., 2022). Previous studies have demonstrated that ethyl acetate exhibits
198 notable fragmentation, resulting in interference at m/z 61 (e.g. C₂H₄O₂H⁺) and m/z 43
199 (e.g. C₂H₂OH⁺) (Haase et al., 2012; de Gouw and Warneke, 2007; Rogers et al.,
200 2006; Fortner et al., 2009). Therefore, we employed the PTR-ToF-MS to directly
201 measure high-purity ester chemicals and identify the characteristic product ions
202 produced by esters under H₃O⁺ and NO⁺ chemical ionization. Several common esters
203 including methyl acetate, ethyl acetate, isopropyl acetate, and vinyl acetate, were
204 selected to investigate instrument fragmentation under different ionizations. As shown
205 in Table. S5, it is intriguing to observe that high-molecular-weight acetates tend to
206 exhibit more fragmentation, resulting in interference at m/z 61 (e.g. C₂H₄O₂H⁺) and m/z
207 43 (e.g. C₂H₂OH⁺). Methyl acetate (95%) and ethyl acetate (72%) displayed limited
208 fragmentation in the instrument, while isopropyl acetate accounted for only 13% of the
209 C₃H₁₀O₂H⁺ ions. Additionally, esters with different chemical structures may undergo
210 distinct modes of fragmentation. For example, vinyl acetate primarily fragmented to
211 produce interfering fragments at m/z 43 (e.g. C₂H₂OH⁺) with a fraction of 78%.
212 Furthermore, considering the PTR-ToF-MS mass spectra from various industrial VCP
213 sources, it is conceivable that other ester compounds might also contribute to these mass
214 channels, emphasizing the need for cautious consideration of m/z 61 (e.g. C₂H₄O₂H⁺)
215 and m/z 43 (e.g. C₂H₂OH⁺) signals measured by H₃O⁺ PTR-ToF-MS in industrial VCP
216 sources. The use of NO⁺ chemical ionization exhibits various reaction pathways with
217 ROGs (Wang et al., 2020; Chen et al., 2022), which can partially mitigate interference
218 from fragment ions (Table. S5). The identified results of acetates based on NO⁺
219 ionization demonstrated considerable improvements for methyl acetate (83%) and ethyl
220 acetate (80%), whereas vinyl acetate exhibited more fragmentation, with the largest



221 contribution (47%) at m/z 43 (e.g. $C_2H_2OH^+$). This result could be explained by the
222 instrument was more likely to have a fracture reaction due to the chemical structure of
223 vinyl acetate, which contains a C=C bond.

224 Additionally, it is challenging to calibrate isopropanol in the H_3O^+ PTR-ToF-MS
225 since alcohols split off water during ionization (Buhr et al., 2002). To overcome this
226 challenge, we implemented daily calibrations of isopropanol under ambient humidity
227 conditions throughout the campaign (Fig. S3). The NO^+ PTR-ToF-MS was also
228 employed to calibrate isopropanol by identifying the characteristic product ions
229 produced under NO^+ ionization (Table. S5). The dominating product ion of isopropanol
230 was observed at m/z 59 (e.g. $C_3H_7O^+$) (88%), which corresponds to acetone ($C_3H_6OH^+$)
231 ions in the H_3O^+ PTR-ToF-MS. Although the dominant product ion for acetone under
232 NO^+ ionization was observed at m/z 88 (e.g. $C_3H_6O(NO)^+$) (77%), the interfere at m/z
233 59 (e.g. $C_3H_6OH^+$) (23%) was not insignificant. Therefore, the concentration of
234 isopropanol measured by NO^+ PTR-ToF-MS in this campaign has eliminated the
235 influence of acetone. Finally, the good agreement between measurements obtained
236 using PTR-ToF-MS with H_3O^+ and NO^+ chemical ionization throughout the campaign
237 indicates that the NO^+ PTR-ToF-MS can serve as a reliable method for measuring
238 isopropanol and ester species in industrial VCP sources (Fig. S4-S5). Our results
239 demonstrated that the NO^+ PTR-ToF-MS can also provide a complementary approach
240 for characterizing ester species and isopropanol in ambient air as well as emission
241 sources.

242 2.4 Mass spectra similarity analysis

243 We conducted a comprehensive comparison of various ROG emission sources by
244 considering the entire range of species in mass spectra as dimensions in a vector, and
245 calculating the cosine angle (θ) similarity (Humes et al., 2022;Ulbrich et al.,
246 2009;Kostenidou et al., 2009). The angle θ between the two mass spectra (MS_a and MS_b)
247 is given by the following:

$$248 \cos \theta = \frac{MS_a MS_b}{|MS_a||MS_b|} \quad (1)$$

249 The θ angles between two mass spectra is divided into 4 groups, including 0° -



250 15°, 15°-30°, 30°-50°, and >50°, which correspond to excellent consistency, good
251 consistency, many similarities, and poor consistency, respectively. Due to the distinct
252 ionization methods of the instruments, our classification of angle similarity is not as
253 strict as that reported in previous studies (Kostenidou et al., 2009; Zhu et al., 2021),

254 **3. Results and discussions**

255 **3.1 Time-resolved ROG emissions from industrial VCP sources**

256 Time series of several ROGs measured by the H₃O⁺ PTR-ToF-MS from five
257 industrial VCP sources are shown in Fig. 1 and Fig. S6. More information for these
258 sources can be found in Sect. S1 in the Supplement. Online measurements were carried
259 out in semi-open workshops (workshops emission) and from ROG treatment devices
260 (i.e. before and after treatment emission). Typically, workshop waste gases are routed
261 through collection devices, followed by collection and treatment in ROG treatment
262 devices, before being released into the atmosphere via exhaust stacks. ROG treatment
263 devices are implemented to reduce ROG emissions after treatment, thereby ensuring
264 that the ROG concentrations after treatment are generally lower than those before
265 treatment. As the waste gas was directly discharged into the ambient after treatment,
266 the after treatment emission was considered as stack emission (Zheng et al., 2013). The
267 average concentrations of eight representative ROGs, including aromatics, ketones,
268 alcohols, and esters, between workshops emission and stack emission for all factories
269 is presented in Fig. S7. The evaluation of the ROGs treatment efficiency is based on the
270 analysis of emission characteristics before and after treatment in the ROG treatment
271 devices, which is discussed in greater detail in Section 3.3. Along with the typical ROGs,
272 the PTR-ToF-MS measured a wide range of ions in abundance in the mass spectra. Fig.
273 2 displays mass spectra representing the average concentrations of stack emissions from
274 five industrial VCP sources for all detected ROGs. These ROGs measured by the PTR-
275 ToF-MS were categorized based on their chemical formula, namely hydrocarbon
276 species (C_xH_y), OVOCs (C_xH_yO₁, C_xH_yO₂, and C_xH_yO_{≥3}), species containing nitrogen
277 and/or sulfur atoms (N/S-containing), species containing siloxanes (Si-containing), and
278 other ions (others).



279 Real-time concentrations of toluene, acetone, ethyl acetate, and isopropanol from
280 the shoemaking industry are displayed in Fig. 1a. The variable manufacturing processes
281 conditions are demonstrated by inconsistent emission levels in the workshops. This
282 variation may be attributed to different emission intensities during different periods.
283 Notably, the significant emissions from the shoemaking industry are primarily
284 attributed to a few low-molecular-weight OVOCs (Fig. 2a), including acetone, MEK,
285 isopropanol, and formaldehyde, followed by a fraction of hydrocarbon species (e.g.
286 toluene). Our results align with previous findings (Zheng et al., 2013; Zhao et al., 2018a),
287 emphasizing that raw chemicals used during the industrial activities play crucial roles
288 in determining the constituents of the industrial VCP emissions.

289 Significant variations in ROG concentrations were also observed from the plastic
290 surface coating industry (Fig 1b). These variations could be attributed to different
291 manufacturing process conditions and the use of different chemicals in workshops as
292 well. As shown in Fig. 2b, OVOCs contribute significantly to emissions from this
293 industry. Representative OVOCs for $C_xH_yO_1$ ions consist of isopropanol, acetone,
294 formaldehyde, methanol, and cyclohexanone. $C_xH_yO_2$ ions refer to acetates and
295 acrylates such as $C_3H_6O_2$ (e.g. methyl acetate), $C_6H_{12}O_2$ (e.g. butyl acetate), $C_9H_{16}O_2$
296 (e.g. allyl hexanoate) and $C_{12}H_{20}O_2$ (e.g. linalyl acetate). Notably, there are some
297 differences from the main components compared to previous results (Zhong et al.,
298 2017), which may be attributed to the substitution of solvent-borne chemicals with
299 water-borne chemicals in industrial VCPs. Moreover, the utilization of PTR-ToF-MS
300 enabled the identification of additional important OVOCs, thereby improving the
301 characterization of ROG emissions from the industrial VCPs.

302 Due to the wide variety of industrial coatings used in the furniture coating
303 industry, numerous ROGs can be observed in the measured mass spectra (Fig. 2c).
304 Notably, $C_xH_yO_2$ (24%) and $C_xH_yO_3$ ions (9%) contribute significantly in this industry.
305 Among the identified species, C_8 aromatics exhibit the highest concentrations,
306 consistent with previous research from industries utilizing solvent-borne coatings (Yuan
307 et al., 2010; Wu et al., 2020b; Wang et al., 2014). Other OVOCs such as MEK, ethanol,



308 and formaldehyde for $C_xH_yO_1$ ions, $C_6H_{12}O_2$ (e.g. butyl acetate), $C_5H_8O_2$ (e.g. methyl
309 methacrylate, acetylacetone) for $C_xH_yO_2$ ions, and $C_6H_{12}O_3$ (e.g. propylene glycol
310 methyl ether acetate, PGMEA) and $C_7H_{14}O_3$ (e.g. butyl lactate) for $C_xH_yO_3$ ions had
311 been found may be associated with emissions from water-borne coatings. This finding
312 underscores the importance of considering high-molecular-weight OVOCs in this
313 industry, further emphasizing the ability of PTR-ToF-MS to better characterize these
314 important OVOCs that serve as raw chemicals for industrial VCPs.

315 Moreover, by employing online PTR-ToF-MS technology, we can gain deeper
316 insights into the emission characteristics of ROGs during both working and non-
317 working hours. We conducted an analysis of ROG emissions in the furniture coating
318 factory during non-working hours (from 10:00 p.m. to 8:00 a.m. the next day) and
319 compared them with emissions during working hours (Fig. 1c). Most ROGs exhibited
320 a gradual decrease in concentration during non-working hours, with the exception of
321 formaldehyde which maintained a constant concentration. Notably, the concentrations
322 of other typical ROGs, such as MEK and C_8 aromatics, were 2-5 times lower during
323 non-working hours compared to working hours. This observation suggests that ROGs
324 may still be emitted even when the painting activities in the factory is halted, with night-
325 time emissions accounting for approximately 20% of total daily emissions. The θ angles
326 of mass spectra between real-time concentrations versus working hours shows that
327 ROG emissions are many similarities during both working and non-working hours (Fig.
328 1d, $\theta < 30^\circ$ in most times). Given that some ROGs were still more abundant and
329 continued to be released into the atmosphere even during non-working hours (e.g. from
330 the volatilization of chemicals), the ROG emissions in factories during non-working
331 hours should not be ignored.

332 The real-time concentrations of typical ROGs measured from the printing
333 industry is shown in Fig. S6a, with an emphasize on the performance of two different
334 ROG treatment devices, namely activated carbon adsorption combined with ultraviolet-
335 ray (UV) photolysis devices and catalytic combustion devices (specifically,
336 regenerative thermal oxidizer (RTO) devices) installed in this factory. Isopropanol was



337 found to have the highest concentration in the printing industry (Fig. 2d), which is
338 consistent with previous studies (Zheng et al., 2013). The higher concentrations of other
339 typical species, such as $C_4H_8O_2$ (e.g. ethyl acetate), $C_5H_{10}O_2$ (e.g. isopropyl acetate),
340 and $C_7H_{16}O_3$ (e.g. dipropylene glycol methyl ether, DPM) substantiate the correlation
341 between ROG emissions and industrial inks utilized in the printing industry. It was
342 found that ROG treatment devices exhibit varying treatment efficiencies for ROGs,
343 particularly for OVOCs (such as isopropanol and ethanol), that may not have been
344 effectively removed by these treatment devices.

345 In comparison to other industrial VCP sources, the ship coating industry exhibits
346 the highest emissions of hydrocarbons (86%), specifically C_6 - C_{11} aromatics (Fig. 2e,
347 also in Fig. S6b, Sect. S1). This may be attributed to the utilization of solvent-borne
348 industrial coatings for ship coating remains prevalent due to stringent requirements for
349 anti-rust and anti-corrosion properties (Malherbe and Mandin, 2007). A few OVOCs,
350 such as methanol and MEK, were identified as significant emissions. These results
351 confirm that ROG emissions from solvent-borne coatings, predominantly composed of
352 C_8 aromatics, continue to be the primary contributors in the ship coating industry, which
353 is consistent with a previous study conducted in the PRD region (Zhong et al., 2017).

354 Fig. 2 provides a quantified of the proportions of different ion categories
355 measured by the PTR-ToF-MS across various industrial VCP sources as well. OVOCs
356 make up the largest fractions in the printing (94%), plastic surface coating (90%),
357 shoemaking (84%), and furniture coating (68%) industries, while they only account for
358 13% of emissions from the ship coating industry. The fractions of different OVOC
359 groups exhibit a general decline from $C_xH_yO_1$ to $C_xH_yO_{\geq 3}$, and OVOCs with more
360 than two oxygen atoms are present in small proportions (0.3%-8.5%) in all industrial
361 VCP sources except for the furniture coating industry (33%), indicating little emissions
362 of these species. However, although these OVOCs with two or more oxygen atoms do
363 not contribute significantly to the overall emissions, some of them may serve as tracer
364 compounds for particular emission sources as they were only detected in single source.
365 Previous studies have identified octamethylcyclotetrasiloxane (D_4 siloxane), texanol



366 (C₁₂H₂₄O₃) and para-chlorobenzotrifluoride (PCBTF, C₇H₄ClF₃) as tracer compounds
367 for individual chemicals (adhesives and coatings) in U.S. cities (Gkatzelis et al., 2021a).
368 We also observed that the concentrations of texanol and PCBTF emitted by relevant
369 industrial VCP sources were unique and almost non-existent in other sources. Texanol
370 was only detected in samples from the plastic surface coating and furniture coating
371 industries that utilize water-borne coatings. Similarly, PCBTF was only found in
372 samples from the ship coating and furniture coating industries that use solvent-borne
373 coatings. These findings suggest that texanol and PCBTF may be applicable as tracer
374 compounds for industrial VCPs in China. On the contrary, D₄ siloxane was not found
375 to be specific to emissions from adhesive-related industrial (i.e. shoemaking industry)
376 (Fig. 1), indicating that D₄ siloxane may not be an appropriate tracer compounds for
377 identifying industrial VCPs in China.

378 **3.2 Distributions of ROG emissions, OHR, OFP, and volatility**

379 We compared the mass spectra of these industrial VCP sources and calculating
380 the θ angles similarity (Fig. 3) (Table. S6). The ROG_s showed a diverse similarity
381 among different types of industrial VCP sources. Only plastic surface coating industry
382 versus printing industry demonstrated good consistency (27°), other mass spectra
383 exhibited poor consistency ($\theta > 60^\circ$). Combined with mass spectra of vehicular
384 emissions (Wang et al., 2022), the θ angle similarities among the mass spectra of
385 industrial VCP sources (62°-90°) were worse than those of vehicular emissions (41°-
386 75°) (Fig. 3). It is interesting to observe that the θ angle similarity among the mass
387 spectra in different workshops in printing and ship coating industries ranged from 1.6°
388 to 9.0° (Table. S7), similar to the mass spectra in various emission standards for
389 gasoline vehicles (4.9°-17°) (Table. S8). Conversely, the θ angle similarity among the
390 mass spectra of workshops in other industrial VCP sources ranged from 13° to 60°,
391 indicating significant differences in ROG emissions from industrial VCP sources. These
392 substantial differences indicate that ROG emissions from industrial VCPs are more
393 complex and diverse than vehicular emissions. Consequently, a more accurate
394 classification of industrial VCP emissions is necessary, as they cannot be directly



395 unified as a single class of emission sources.

396 The combination of PTR-ToF-MS and canister-GC-MS/FID measurements
397 allowed for more comprehensive speciation of ROG emissions from industrial VCP
398 sources. This comprehensive approach enabled the determination of the fractions of
399 ROGs in total ROG emissions for various industrial VCP sources (Table. S9, Fig. S5,
400 details in Sect. S2 in the Supplement). Additionally, ROGs reactivity plays a crucial
401 role in characterizing the contributions of different ROGs to atmospheric chemical
402 reactions and the formation of secondary pollutants (Wu et al., 2020a; Yang et al., 2016).
403 The overall OHR of ROGs was calculated to comprehend the role of ROGs emitted by
404 industrial VCP sources. The calculation only employed ROGs with known reaction rate
405 constants with the OH radical, which were taken from previous studies (Atkinson and
406 Arey, 2003; Atkinson et al., 2004; Atkinson et al., 2006; Koss et al., 2018; Wu et al.,
407 2020a; Zhao et al., 2016). The fractions of ROGs in the total OHR of ROGs can be
408 determined for various industrial VCP sources (Table. S10). ROGs are grouped into
409 categories, including OVOCs, N/S-containing, and heavy aromatics and monoterpenes
410 measured by H₃O⁺ PTR-ToF-MS, higher alkanes (including C₁₀-C₂₀ acyclic, cyclic, and
411 bicyclic cycloalkanes) measured by NO⁺ PTR-ToF-MS, and alkanes, alkenes, aromatics,
412 and halohydrocarbons measured by canister-GC-MS/FID.

413 OVOCs contributed significantly to total ROG emissions (Fig. 4a), and fractions
414 of OVOCs in total ROG emissions are comparable to previous studies (Fig. 5). Notably,
415 OVOCs account for 67% of total ROG emissions from the shoemaking industry, which
416 is slightly lower than findings from other studies in the PRD region (Zheng et al., 2013)
417 but higher than those reported in previous studies (Zhou et al., 2020a; Zhao et al., 2018a).
418 The fractions of OVOCs in total ROG emissions from plastic surface coating, printing,
419 and furniture coating industries are 96%±0.2%, 85%±6.5%, and 77%, respectively.
420 Compared to previous studies (Zhong et al., 2017; Zheng et al., 2013; Fang et al.,
421 2019; Zhao et al., 2018a; Wang et al., 2019; Zhou et al., 2020a; Zhao et al., 2021),
422 determined OVOC fractions for these industrial VCP sources are much higher (Fig. 5),
423 which may be related to two reasons: (1) more OVOC species are detected in this study;



424 (2) water-borne coatings and inks are more widely employed in the recent year which
425 may enhance OVOC fractions. Moreover, OVOCs account for $16\% \pm 3.5\%$ of total ROG
426 emissions from the ship coating industry by using the solvent-borne coatings, and the
427 fraction is also higher than findings from in one previous study (Zhong et al., 2017).
428 Additionally, OVOCs also contribute to the largest fraction in total OHR of ROGs from
429 all industrial VCP sources (72%-97%) except for the ship coating industry ($15\% \pm 3.6\%$)
430 (Fig. 4b). In contrast to the important contribution of OVOCs, the fractions of
431 hydrocarbons measured by canister-GC-MS/FID only made considerable contributions
432 in specific industrial VCP sources (Fig. 4). For instance, aromatics were found to be the
433 major contributors to both total ROG emissions and OHR in the ship coating industry,
434 making up $74\% \pm 6.1\%$ and $79\% \pm 4.8\%$ respectively. Alkanes measured by canister-GC-
435 MS/FID only make contributions in the shoemaking industry, comprising 26% of the
436 total ROG emissions. Overall, the total OHR of ROGs was dominated by OVOCs and
437 aromatics, and the contributions of other species were in the range of 1.8%-21% (Fig.
438 4b). These results stress the importance of measuring a broad range of OVOCs using
439 PTR-ToF-MS in characterizing ROG emissions from industrial VCP sources.

440 The application of NO^+ PTR-ToF-MS provided the opportunity for detecting
441 emissions of higher alkanes from industrial VCP sources. We show that the contribution
442 of higher alkanes can be significant for VCP sources. Specifically, the printing industry
443 demonstrates a noteworthy presence of higher alkanes, accounting for $27\% \pm 2.7\%$ and
444 $8.2\% \pm 2.4\%$ in workshop and stack emissions, respectively (Table. S9). This can be
445 attributed to the use of lubricating oil, a primary component of industrial inks, which
446 contains substantial amounts of alkanes (Liang et al., 2018). Furthermore, emissions
447 from forklifts transporting products in printing workshops also contribute to the
448 emission of higher alkanes (Li et al., 2021), suggesting non-road vehicles may
449 contribute to the emissions from industrial VCP factories. In addition, the fractions of
450 higher alkanes in stack emission are lower than in workshops, suggesting that ROG
451 treatment devices effectively reduce emissions of higher alkanes.

452 To facilitate for making controlling strategies for ozone, we determine the ozone



453 formation potential for a unity of emission from different sources for comparison (Yuan
454 et al., 2010; Na and Pyo Kim, 2007), which represent the ability to ozone formation
455 from ROG sources on a relative basis (Fig. 6) Our calculations specifically focused on
456 ROGs with known maximum incremental reactivity (MIR) values, derived from
457 previous studies (Carter, 2007). Among the industrial VCP sources considered, the ship
458 coating industry exhibited the highest OFP, reaching as high as $5.5 \text{ g O}_3 \cdot \text{g}^{-1} \text{ ROGs}$,
459 followed by the furniture coating industry, with a value of $2.7 \text{ g O}_3 \cdot \text{g}^{-1} \text{ ROGs}$. The OFP
460 for other industrial VCP sources ranged from $0.79 \text{ g O}_3 \cdot \text{g}^{-1} \text{ ROGs}$ to $1.4 \text{ g O}_3 \cdot \text{g}^{-1} \text{ ROGs}$.
461 Among all industrial VCP sources, aromatics (ranging from 4.2% to 91%) and OVOCs
462 (ranging from 6.7% to 94%) were identified as the primary contributors to OFP.
463 Compared to vehicular emissions, the OFP from the ship coating and furniture coating
464 industries are significantly higher (Fig. 5), suggesting that these sources should be
465 controlled in priority. Given the higher reactivity value for ship coating industry relative
466 to other sources, it is evident that controlling ROG emissions from solvent-borne
467 industrial chemicals would have a more substantial impact on reducing ozone formation
468 compared to other sources. Moreover, it is important to note that the emissions of
469 solvent-borne chemicals surpass those of vehicles, while water-borne chemicals have
470 lower emissions compared to vehicles. This observation implies that the substitution of
471 solvent-borne chemicals with water-borne chemicals in China holds considerable
472 importance in mitigating and controlling ozone pollution.

473 We further compare centralization for species among different ROGs sources by
474 determining the contribution from the top ten species in terms of concentrations, OHR,
475 and OFP (Fig. 7 and Fig S8, also in Table S11). We show that the top ten ROGs account
476 for over 50% on ROG emissions, OHR, and OFP (Fig. 7). With the exception of
477 furniture coating industry, the fractions on the top ten species in total emissions, OHR,
478 and OFP from industrial VCP sources were in range of 89%-96%. The lower fractions
479 (ranging from 69% to 86%) of the top ten species in the furniture coating industry may
480 be a result of the wider range of industrial coatings (i.e. both solvent-borne and water-
481 borne coatings) utilized in this industry. ROGs emitted from industrial VCP sources are



482 apparently more centralized compared to vehicular emissions (ranging from 51% to
483 87%). Additionally, the cumulative fractions of the top one hundred species in overall
484 ROG emissions, OHR, and OFP in various industrial VCP sources is further indicated
485 the highly centralized of ROG emissions from various emission sources (Fig. S8). More
486 than half of the top ten species in ROG emissions, OHR, and OFP from industrial VCP
487 sources were OVOCs (Table S11). Among them, isopropanol made a notable
488 contribution to the printing, plastic surface coating, and shoemaking industries. Other
489 OVOCs such as MEK, acetone, and ethyl acetate contributed to total ROG emissions
490 in each industry, while formaldehyde, acetaldehyde contributed to total OHR and OFP.
491 It should be noted that the proportions of C₁₃, C₁₄, and C₁₅ cycloalkanes from printing
492 industry (account for 6.3% in ROG emissions), as well as the proportion of C₁₁
493 aromatics from ship coating industry (account for 1.0% in ROG emissions) are not
494 negligible. Additionally, acetylacetone is a common species with broad industrial
495 applications, and contributes importantly to secondary pollutants formation under
496 polluted environments (Ji et al., 2018). Although it only contributes 8.7% to total
497 emissions from the furniture coating industry, its fraction in terms of total OHR can be
498 as high as 30%. These findings demonstrated that previously underreported ROGs
499 should receive greater attention in future research.

500 The updated measurements of OVOC emissions by using the PTR-ToF-MS
501 substantially improve our understanding of the emission of industrial VCP sources. The
502 effective saturation concentrations (C*) of high-molecular-weight OVOCs were found
503 to be lower, which were corresponding to intermediate-volatility organic compounds
504 (IVOCs) and semi-volatile organic compounds (SVOCs). Since these S/I-VOCs are
505 crucial precursors for the SOA in urban environments (Zhao et al., 2014), it is important
506 to comprehend their contributions from the emissions of industrial VCP sources across
507 various volatility classes, including volatility organic compounds (VOCs), IVOCs, and
508 SVOCs (Guenther et al., 2012; Li et al., 2016). Fig. 8 illustrates the distribution of ROG
509 species in a two-dimensional volatility basis set (2D-VBS) space for various industrial
510 VCP sources, categorized based on volatility bins (Li et al., 2016; Donahue et al., 2011).



511 It is worth noting that the volatility distributions exhibit substantial variation across
512 industrial VCP sources (Fig. 8a). Generally, VOCs constitute the predominant fraction
513 of emissions from industrial VCP sources, accounting for 59% to 98% of the total
514 emissions. The fractions of IVOCs are largest in the printing industry (40%), compared
515 to the range of 2.1%-9.6% in other industrial VCP sources. Conversely, the contribution
516 of SVOCs from industrial VCP sources are negligible in our study, accounting for less
517 than 1%. Considering the importance of S/I-VOCs in SOA formation, particularly with
518 the increasing adoption of improved online mass spectrometry technologies, the S/I-
519 VOCs emissions from industrial VCP sources should be paid more attention in future
520 research.

521 **3.3 Evaluate ROGs treatment efficiency in industrial VCP sources**

522 The analysis of the PTR-ToF-MS mass spectra offers valuable insights into the
523 impact of ROG emissions from industrial VCP sources. This comprehensive
524 information provided by the PTR-ToF-MS also allows for a systematic comparison of
525 emissions before and after the treatment of ROGs. ROG treatment devices are
526 employed to reduce ROG emissions after treatment. Here, we evaluate two types of
527 ROG treatment devices: activated carbon adsorption combined with UV photolysis
528 devices (installed in shoemaking, plastic surface coating, furniture coating, and printing
529 industries) and catalytic combustion devices (installed in printing and ship coating
530 industries).

531 The scatterplot of the concentrations of various ROG before and after treatment
532 in industrial VCP sources are shown in Fig. 9. The observed treatment efficiency,
533 represented by 1-slope, did not reach the desired levels, ranging from -12% to 68%.
534 Among the industrial VCP sources investigated, the shoemaking industry exhibited the
535 highest treatment efficiency (slope=0.32) with the activated carbon adsorption
536 combined with UV photolysis device. This remarkable efficiency can be attributed to
537 the large-scale nature of the factory and meticulous regulation of the ROG treatment
538 devices. Following closely behind is the printing industry, utilizing catalytic
539 combustion devices, with a slightly higher efficacy (slope=0.67) than another treatment



540 device in the same factory (slope=0.80). However, it is evident that the treatment
541 efficiency has not reached the desired levels, possibly due to the challenges associated
542 with effectively removing OVOC emissions from the printing industry using current
543 treatment technologies. Additionally, we also observed that some OVOCs may be
544 generated as byproducts after the implementation of treatment devices in printing
545 industry. For instance, the concentrations of CH_2O_2 (e.g. formic acids), $\text{C}_4\text{H}_6\text{O}_3$ (e.g.
546 propylene carbonate), and $\text{C}_9\text{H}_{18}\text{O}$ (e.g. nonanal) were found to be higher after the
547 application of activated carbon adsorption combined with UV photolysis devices (Fig.
548 9d). Similarly, the concentrations of $\text{C}_3\text{H}_4\text{O}$ (e.g. acrolein) and $\text{C}_{12}\text{H}_{18}\text{O}_4$ (e.g. dibutyl
549 squarate) were also higher following the utilization of catalytic combustion devices (Fig.
550 9e). Therefore, it is crucial to consider the potential contribution of these ROG when
551 assessing the emissions released into the atmosphere. The lowest treatment efficiency
552 of ROG was shown in the furniture coating industry (slope=1.12). This potentially
553 attributed to the ineffective performance of the ROG treatment devices in this particular
554 facility, as activated carbon and other adsorption materials were not promptly replaced.

555 Furthermore, the θ angles between the mass spectra of ROG from workshops,
556 before and after ROG treatment devices for various industrial VCP sources were
557 calculated and summarized in Fig. S9 (also in Table. S12). A comparison between the
558 correlation of mass spectra among workshops versus after treatment devices (ranging
559 from 6.2° to 49°) and workshops versus before treatment devices (ranging from 4.2° to
560 41°) demonstrated a poorer correlation in the former case. The similarities between
561 workshops and stack emissions in the shoemaking industry were lower compared to
562 other industrial VCP sources. This discrepancy can potentially be attributed to the
563 inclusion of ROG emissions from non-VCP usage manufacturing processes (e.g. sole
564 injection molding) in the collection process of ROG treatment devices. Additionally,
565 the θ angles similarity between the mass spectra from before and after ROG treatment
566 devices in various industrial VCP sources also providing insight into the efficacy of the
567 devices in removing ROG (Fig. 9). The θ angles in ROG treatment devices from five
568 industrial VCP sources were found to range from 1.8° to 27° , indicating good



569 consistency between the mass spectra before and after treatment of ROGs. This
570 alignment suggests that the chemical compositions of ROG emissions remain
571 comparable before and after treatment ($R \geq 0.87$), implying that the relative proportions
572 of various ROG components are not significantly affected by the ROG treatment
573 devices in these industrial VCP sources.

574 **3.4 Comparison of industrial VCP sources and ambient air**

575 To gain deeper insights into the atmospheric impact of emissions from industrial
576 VCP sources, an in-situ measurement was carried out at a monitoring station nearby the
577 furniture coating industry, located 2 km northeast from the industry site. The
578 measurement was conducted using a PTR-ToF-MS (Kore Inc., U.K.), which enabled
579 the quantification of various common ROGs. More information about this instrument
580 and dataset for in-situ measurement can be found elsewhere (Gonzalez-Mendez et al.,
581 2016; Song et al., 2023). Concordant with expectations, the average concentrations of
582 representative ROGs generally demonstrate a discernible decline from the furniture
583 coating industry (including stack emission and workshops during working and non-
584 working hours) to the monitor station (Fig. 10). C_8 aromatics and MEK performed
585 considerable emissions from furniture coating industry, while the concentrations of
586 them in the ambient air are orders of magnitude lower than those observed in the
587 industry. However, ambient concentrations of OVOCs, specifically MEK (6.8 ± 8.2 ppb)
588 and ethyl acetate (7.5 ± 5.9 ppb) are still significantly higher than clean environments
589 and are among the highest measured concentration in the literature (Wu et al., 2020a; He
590 et al., 2022b; Khare et al., 2022; Yang et al., 2022). It is confirmed that OVOCs should
591 be paid attention to in industrialized urban areas, thereby further substantiating the
592 significance of OVOC emissions from industrial VCP sources to atmospheric pollution.
593 These results stress the invaluable insights provided by PTR-ToF-MS in
594 comprehensively characterizing ROG compositions in both emission sources and urban
595 air.

596 The preceding discussions illustrate that the emission characteristics of ROGs
597 significantly vary among industrial VCP sources. As a result, the ratio of ROG pairs



598 can be used to distinguish emissions of industrial VCP sources. MEK and C₈ aromatics
599 emerge as key species in industrial VCP emissions, and the reaction rate constants of
600 C₈ aromatics with OH radical ($k_{OH} = (1.4-2.3) \times 10^{-11} \text{ cm}^3 \cdot \text{molecule}^{-1} \cdot \text{s}^{-1}$) are higher
601 than MEK ($k_{OH} = 5.5 \times 10^{-12} \text{ cm}^3 \cdot \text{molecule}^{-1} \cdot \text{s}^{-1}$) (Atkinson and Arey, 2003; Wu et al.,
602 2020a). Fig. 11 illustrates the correlation of MEK with C₈ aromatics in stack emission,
603 workshops during working hours and non-working hours in the furniture coating
604 industry, as well as ambient measurement near the industry. Positive correlations
605 between MEK and C₈ aromatics are observed in both emission sources and ambient
606 measurements, indicating a shared source for these compounds. Additionally, the
607 observed ratios of MEK to C₈ aromatics in ambient measurement are also comparable
608 with the ratios of MEK to C₈ aromatics measured in emissions from the furniture
609 coating industry (0.97 ppb·ppb⁻¹ for the stack emission and 0.75 ppb·ppb⁻¹ for the
610 workshops emission), suggesting that industrial VCP emissions (specifically furniture
611 coating) may account for the enhancement of MEK and C₈ aromatics in this industrial
612 area. Thus, the divergence in MEK / C₈ aromatics ratio among different industrial VCP
613 sources suggests that these ratios could serve as effective indicators for distinguishing
614 industrial VCP emissions, particularly in ambient measurements within industrial areas.
615 Consequently, the MEK to C₈ aromatics ratio could provide an additional tracer for
616 assessing the contribution of industrial VCP emissions by using high time-resolution
617 ROG measurements from PTR-ToF-MS.

618 **4. Conclusion**

619 In this work, we conducted a field campaign to measure more comprehensive
620 speciation of ROG emissions from industrial VCP sources, including shoemaking,
621 plastic surface coating, furniture coating, printing, and ship coating industries. To
622 achieve this, we employed the PTR-ToF-MS in combination with canister-GC-MS/FID
623 techniques. Our study identified OVOCs had been identified as representative ROGs
624 emitted from these sources, which are highly related to specific chemicals used during
625 the industrial activities. Furthermore, we performed a mass spectra similarity analysis
626 to compare the ROG emissions across different emission sources. The poor consistency



627 of the similarity between the mass spectra in emission sources indicating that substantial
628 differences between industrial VCP sources, as they cannot be directly categorized as a
629 single class of emission sources.

630 In addition, the fractions of ROG_s in total ROG emissions and OHR are
631 determined by combining measurements from canister-GC-MS/FID and PTR-ToF-MS.
632 Except for the ship coating industry utilizing solvent-borne coatings, the proportions of
633 OVOCs range from 67% to 96% in total ROG emissions and 72% to 97% in total OHR
634 for different industrial sources. Large fraction of OVOCs may be related to two reasons:
635 (1) more OVOC species are detected in this study; (2) water-borne coatings and inks
636 are more widely employed in the recent year which may enhance OVOC fractions. This
637 highlights the importance of measuring these OVOC emissions from industrial VCP
638 sources. The industrial VCP sources associated with solvent-borne coatings exhibited a
639 higher OFP, reaching as high as 5.5 and 2.7 g O₃·g⁻¹ ROG_s for ship coating and
640 furniture coating industries, primarily due to contributions from aromatics, suggesting
641 that these sources should be controlled in priority. The fractions of the ten most
642 abundant species in total ROG emissions, OHR, and OFP indicate the highly centralized
643 of ROG emissions from various emission sources.

644 Our results suggest that ROG treatment devices may have limited effectiveness
645 in removing ROG_s, with treatment efficiencies ranging from -12% to 68%. In addition,
646 the average concentrations of representative ROG_s generally demonstrate a downward
647 trend from emission sources to the ambient air. Our results demonstrate that ROG
648 pairs (e.g., MEK / C₈ aromatics ratio) can be utilized as reliable indicators for
649 distinguishing industrial VCP sources, particularly for measurements in industrial areas.

650 This study highlights the significant role of OVOCs to ROG emissions from
651 industrial VCP sources, particularly those utilizing water-borne chemicals. As a result,
652 these industrial VCP sources may significantly contribute to the primary emissions of
653 OVOCs in urban regions. The current emission inventories do not fully account for the
654 emissions of many ROG_s, which can compromise the predictive accuracy of air quality
655 models in urban areas. In this study, a broader range of ROG species was quantified



656 using PTR-ToF-MS measurements, which highlights the effectiveness of PTR-ToF-MS
657 in characterizing ROG emissions from industrial VCP sources..

658

659 **Data availability**

660 Data are available from the authors upon request.

661 **Author contribution**

662 BY designed the research. BY and SHW organized industrial VCP source
663 measurements. SHW, XJH, RC, CHW, and CMW contributed to data collection. SHW
664 performed the data analysis, with contributions from XS and YBC. SHW and BY
665 prepared the manuscript with contributions from YBH, XBL, BGW and MS. All the
666 authors reviewed the manuscript.

667 **Competing interests**

668 The authors declare that they have no known competing financial interests or
669 personal relationships that could have appeared to influence the work reported in this
670 paper.

671 **Acknowledgement**

672 This work was supported by the National Key R&D Plan of China (grant No.
673 2022YFC3700604), the National Natural Science Foundation of China (grant No.
674 42230701). This work was also Supported by the Outstanding Innovative Talents
675 Cultivation Funded Programs for Doctoral Students of Jinan University (grant
676 No.2022CXB028).

677



678 **References**

- 679 Atkinson, R., and Arey, J.: Atmospheric Degradation of Volatile Organic Compounds,
680 Chemical Reviews, 103, 4605-4638, 10.1021/cr0206420, 2003.
- 681 Atkinson, R., Baulch, D. L., Cox, R. A., Crowley, J. N., Hampson, R. F., Hynes, R. G.,
682 Jenkin, M. E., Rossi, M. J., and Troe, J.: Evaluated kinetic and photochemical data for
683 atmospheric chemistry: Volume I - gas phase reactions of Ox, HOx, NOx and SOx
684 species, Atmos. Chem. Phys., 4, 1461-1738, 10.5194/acp-4-1461-2004, 2004.
- 685 Atkinson, R., Baulch, D. L., Cox, R. A., Crowley, J. N., Hampson, R. F., Hynes, R. G.,
686 Jenkin, M. E., Rossi, M. J., Troe, J., and Subcommittee, I.: Evaluated kinetic and
687 photochemical data for atmospheric chemistry: Volume II – gas phase reactions
688 of organic species, Atmos. Chem. Phys., 6, 3625-4055, 10.5194/acp-6-3625-2006, 2006.
- 689 Buhr, K., van Ruth, S., and Delahunty, C.: Analysis of volatile flavour compounds by
690 Proton Transfer Reaction-Mass Spectrometry: fragmentation patterns and
691 discrimination between isobaric and isomeric compounds, International Journal of
692 Mass Spectrometry, 221, 1-7, [https://doi.org/10.1016/S1387-3806\(02\)00896-5](https://doi.org/10.1016/S1387-3806(02)00896-5), 2002.
- 693 Cappellin, L., Karl, T., Probst, M., Ismailova, O., Winkler, P. M., Soukoulis, C., Aprea,
694 E., Mark, T. D., Gasperi, F., and Biasioli, F.: On quantitative determination of volatile
695 organic compound concentrations using proton transfer reaction time-of-flight mass
696 spectrometry, Environmental Science & Technology, 46, 2283-2290,
697 10.1021/es203985t, 2012.
- 698 Carter, W. P.: Development of the SAPRC-07 chemical mechanism and updated ozone
699 reactivity scales, Citeseer, 2007.
- 700 Chang, X., Zhao, B., Zheng, H., Wang, S., Cai, S., Guo, F., Gui, P., Huang, G., Wu, D.,
701 Han, L., Xing, J., Man, H., Hu, R., Liang, C., Xu, Q., Qiu, X., Ding, D., Liu, K., Han,
702 R., Robinson, A. L., and Donahue, N. M.: Full-volatility emission framework corrects
703 missing and underestimated secondary organic aerosol sources, One Earth, 5, 403-412,
704 <https://doi.org/10.1016/j.oneear.2022.03.015>, 2022.
- 705 Chen, Y., Yuan, B., Wang, C., Wang, S., He, X., Wu, C., Song, X., Huangfu, Y., Li, X.
706 B., Liao, Y., and Shao, M.: Online measurements of cycloalkanes based on NO⁺
707 chemical ionization in proton transfer reaction time-of-flight mass spectrometry (PTR-
708 ToF-MS), Atmos. Meas. Tech., 15, 6935-6947, 10.5194/amt-15-6935-2022, 2022.
- 709 Coggon, M. M., McDonald, B. C., Vlasenko, A., Veres, P. R., Bernard, F., Koss, A. R.,
710 Yuan, B., Gilman, J. B., Peischl, J., Aikin, K. C., DuRant, J., Warneke, C., Li, S. M.,
711 and de Gouw, J. A.: Diurnal Variability and Emission Pattern of
712 Decamethylcyclopentasiloxane (D5) from the Application of Personal Care Products in
713 Two North American Cities, Environ Sci Technol, 52, 5610-5618,
714 10.1021/acs.est.8b00506, 2018.
- 715 Coggon, M. M., Gkatzelis, G. I., McDonald, B. C., Gilman, J. B., Schwantes, R. H.,
716 Abuhassan, N., Aikin, K. C., Arend, M. F., Berkoff, T. A., Brown, S. S., Campos, T. L.,
717 Dickerson, R. R., Gronoff, G., Hurley, J. F., Isaacman-VanWertz, G., Koss, A. R., Li,
718 M., McKeen, S. A., Moshary, F., Peischl, J., Pospisilova, V., Ren, X., Wilson, A., Wu,
719 Y., Trainer, M., and Warneke, C.: Volatile chemical product emissions enhance ozone



720 and modulate urban chemistry, *Proc Natl Acad Sci U S A*, 118,
721 10.1073/pnas.2026653118, 2021.

722 de Gouw, J., and Warneke, C.: Measurements of volatile organic compounds in the
723 earth's atmosphere using proton-transfer-reaction mass spectrometry, *Mass Spectrom*
724 *Rev* 26, 223-257, 10.1002/mas.20119, 2007.

725 Donahue, N. M., Epstein, S. A., Pandis, S. N., and Robinson, A. L.: A two-dimensional
726 volatility basis set: 1. organic-aerosol mixing thermodynamics, *Atmospheric Chemistry*
727 *and Physics*, 11, 3303-3318, 10.5194/acp-11-3303-2011, 2011.

728 Fang, L., Liu, W., Chen, D., Li, G., Wang, D., Shao, X., and Nie, L.: Source Profiles of
729 Volatile Organic Compounds (VOCs) from Typical Solventbased Industries in Beijing
730 (in Chinese), *Environmental Science*, 40, 4395-4403, 10.13227/j.hjlx.201901128,
731 2019.

732 Fortner, E. C., Zheng, J., Zhang, R., Berk Knighton, W., Volkamer, R. M., Sheehy, P.,
733 Molina, L., and André, M.: Measurements of Volatile Organic Compounds Using
734 Proton Transfer Reaction – Mass Spectrometry during the MILAGRO 2006 Campaign,
735 *Atmos. Chem. Phys.*, 9, 467-481, 10.5194/acp-9-467-2009, 2009.

736 Gao, Y., Wang, H., Yuan, L., Jing, S., Yuan, B., Shen, G., Zhu, L., Koss, A., Li, Y., Wang,
737 Q., Huang, D. D., Zhu, S., Tao, S., Lou, S., and Huang, C.: Measurement report:
738 Underestimated reactive organic gases from residential combustion – insights from a
739 near-complete speciation, *Atmospheric Chemistry and Physics*, 23, 6633-6646,
740 10.5194/acp-23-6633-2023, 2023.

741 Gkatzelis, G. I., Coggon, M. M., McDonald, B. C., Peischl, J., Aikin, K. C., Gilman, J.
742 B., Trainer, M., and Warneke, C.: Identifying Volatile Chemical Product Tracer
743 Compounds in U.S. Cities, *Environ Sci Technol*, 55, 188-199, 10.1021/acs.est.0c05467,
744 2021a.

745 Gkatzelis, G. I., Coggon, M. M., McDonald, B. C., Peischl, J., Gilman, J. B., Aikin, K.
746 C., Robinson, M. A., Canonaco, F., Prevot, A. S. H., Trainer, M., and Warneke, C.:
747 Observations Confirm that Volatile Chemical Products Are a Major Source of
748 Petrochemical Emissions in U.S. Cities, *Environ Sci Technol*, 55, 4332-4343,
749 10.1021/acs.est.0c05471, 2021b.

750 Gonzalez-Mendez, R., Watts, P., Olivenza-Leon, D., Reich, D. F., Mullock, S. J., Corlett,
751 C. A., Cairns, S., Hickey, P., Brookes, M., and Mayhew, C. A.: Enhancement of
752 Compound Selectivity Using a Radio Frequency Ion-Funnel Proton Transfer Reaction
753 Mass Spectrometer: Improved Specificity for Explosive Compounds, *Anal Chem*, 88,
754 10624-10630, 10.1021/acs.analchem.6b02982, 2016.

755 Guenther, A. B., Jiang, X., Heald, C. L., Sakulyanontvittaya, T., Duhl, T., Emmons, L.
756 K., and Wang, X.: The Model of Emissions of Gases and Aerosols from Nature version
757 2.1 (MEGAN2.1): an extended and updated framework for modeling biogenic
758 emissions, *Geoscientific Model Development*, 5, 1471-1492, 10.5194/gmd-5-1471-
759 2012, 2012.

760 Haase, K. B., Keene, W. C., Pszenny, A. A. P., Mayne, H. R., Talbot, R. W., and Sive,
761 B. C.: Calibration and intercomparison of acetic acid measurements using proton-
762 transfer-reaction mass spectrometry (PTR-MS), *Atmospheric Measurement Techniques*,
763 5, 2739-2750, 10.5194/amt-5-2739-2012, 2012.



- 764 Han, C., Liu, R., Luo, H., Li, G., Ma, S., Chen, J., and An, T.: Pollution profiles of
765 volatile organic compounds from different urban functional areas in Guangzhou China
766 based on GC/MS and PTR-TOF-MS: Atmospheric environmental implications,
767 *Atmospheric Environment*, 214, 10.1016/j.atmosenv.2019.116843, 2019.
- 768 He, X., Che, X., Gao, S., Chen, X., Pan, M., Jiang, M., Zhang, S., Jia, H., and Duan, Y.:
769 Volatile organic compounds emission inventory of organic chemical raw material
770 industry, *Atmospheric Pollution Research*, 13, 10.1016/j.apr.2021.101276, 2022a.
- 771 He, X., Yuan, B., Wu, C., Wang, S., Wang, C., Huangfu, Y., Qi, J., Ma, N., Xu, W.,
772 Wang, M., Chen, W., Su, H., Cheng, Y., and Shao, M.: Volatile organic compounds in
773 wintertime North China Plain: Insights from measurements of proton transfer reaction
774 time-of-flight mass spectrometer (PTR-ToF-MS), *Journal of Environmental Sciences*,
775 10.1016/j.jes.2021.08.010, 2022b.
- 776 Huang, C., Chen, C. H., Li, L., Cheng, Z., Wang, H. L., Huang, H. Y., Streets, D. G.,
777 Wang, Y. J., Zhang, G. F., and Chen, Y. R.: Emission inventory of anthropogenic air
778 pollutants and VOC species in the Yangtze River Delta region, China, *Atmospheric
779 Chemistry and Physics*, 11, 4105-4120, 10.5194/acp-11-4105-2011, 2011.
- 780 Huangfu, Y., Yuan, B., Wang, S., Wu, C., He, X., Qi, J., de Gouw, J., Warneke, C.,
781 Gilman, J. B., Wisthaler, A., Karl, T., Graus, M., Jobson, B. T., and Shao, M.: Revisiting
782 Acetonitrile as Tracer of Biomass Burning in Anthropogenic-Influenced Environments,
783 *Geophysical Research Letters*, 48, 10.1029/2020gl092322, 2021.
- 784 Humes, M. B., Wang, M., Kim, S., Machesky, J. E., Gentner, D. R., Robinson, A. L.,
785 Donahue, N. M., and Presto, A. A.: Limited Secondary Organic Aerosol Production
786 from Acyclic Oxygenated Volatile Chemical Products, *Environ Sci Technol*, 56, 4806-
787 4815, 10.1021/acs.est.1c07354, 2022.
- 788 Inomata, S., Tanimoto, H., and Yamada, H.: Mass Spectrometric Detection of Alkanes
789 Using NO⁺ Chemical Ionization in Proton-transfer-reaction Plus Switchable Reagent
790 Ion Mass Spectrometry, *Chemistry Letters*, 43, 538-540, 10.1246/cl.131105, 2014.
- 791 Ji, Y., Zheng, J., Qin, D., Li, Y., Gao, Y., Yao, M., Chen, X., Li, G., An, T., and Zhang,
792 R.: OH-Initiated Oxidation of Acetylacetone: Implications for Ozone and Secondary
793 Organic Aerosol Formation, *Environ Sci Technol*, 52, 11169-11177,
794 10.1021/acs.est.8b03972, 2018.
- 795 Khare, P., and Gentner, D. R.: Considering the future of anthropogenic gas-phase
796 organic compound emissions and the increasing influence of non-combustion sources
797 on urban air quality, *Atmospheric Chemistry and Physics*, 18, 5391-5413, 10.5194/acp-
798 18-5391-2018, 2018.
- 799 Khare, P., Krechmer, J. E., Machesky, J. E., Hass-Mitchell, T., Cao, C., Wang, J., Majluf,
800 F., Lopez-Hilfiker, F., Malek, S., Wang, W., Seltzer, K., Pye, H. O. T., Commane, R.,
801 McDonald, B. C., Toledo-Crow, R., Mak, J. E., and Gentner, D. R.: Ammonium adduct
802 chemical ionization to investigate anthropogenic oxygenated gas-phase organic
803 compounds in urban air, *Atmospheric Chemistry and Physics*, 22, 14377-14399,
804 10.5194/acp-22-14377-2022, 2022.
- 805 Koss, A. R., Warneke, C., Yuan, B., Coggon, M. M., Veres, P. R., and de Gouw, J. A.:
806 Evaluation of NO⁺ reagent ion chemistry for online measurements of atmospheric



807 volatile organic compounds, *Atmospheric Measurement Techniques*, 9, 2909-2925,
808 10.5194/amt-9-2909-2016, 2016.

809 Koss, A. R., Sekimoto, K., Gilman, J. B., Selimovic, V., Coggon, M. M., Zarzana, K.
810 J., Yuan, B., Lerner, B. M., Brown, S. S., Jimenez, J. L., Krechmer, J., Roberts, J. M.,
811 Warneke, C., Yokelson, R. J., and de Gouw, J.: Non-methane organic gas emissions
812 from biomass burning: identification, quantification, and emission factors from PTR-
813 ToF during the FIREX 2016 laboratory experiment, *Atmospheric Chemistry and
814 Physics*, 18, 3299-3319, 10.5194/acp-18-3299-2018, 2018.

815 Kostenidou, E., Lee, B.-H., Engelhart, G. J., Pierce, J. R., and Pandis, S. N.: Mass
816 Spectra Deconvolution of Low, Medium, and High Volatility Biogenic Secondary
817 Organic Aerosol, *Environmental Science & Technology*, 43, 4884-4889,
818 10.1021/es803676g, 2009.

819 Li, C., Cui, M., Zheng, J., Chen, Y., Liu, J., Ou, J., Tang, M., Sha, Q., Yu, F., Liao, S.,
820 Zhu, M., Wang, J., Yao, N., and Li, C.: Variability in real-world emissions and fuel
821 consumption by diesel construction vehicles and policy implications, *Sci Total Environ*,
822 786, 147256, 10.1016/j.scitotenv.2021.147256, 2021.

823 Li, G., Jiang, B., Wang, S., Li, C., Yuan, B., Wang, B., and Zhanyi, Z.: Determination
824 of 118 Volatile Organic Compounds in Source Emission by Canister Sampling-
825 Preconcentration /Gas Chromatography – Mass Spectrometry (in Chinese), *Journal of
826 Instrumental Analysis*, 39, 1441-1450, 2020.

827 Li, L., and Cocker, D. R.: Molecular structure impacts on secondary organic aerosol
828 formation from glycol ethers, *Atmospheric Environment*, 180, 206-215,
829 10.1016/j.atmosenv.2017.12.025, 2018.

830 Li, M., Zhang, Q., Zheng, B., Tong, D., Lei, Y., Liu, F., Hong, C. P., Kang, S. C., Yan,
831 L., Zhang, Y. X., Bo, Y., Su, H., Cheng, Y. F., and He, K. B.: Persistent growth of
832 anthropogenic non-methane volatile organic compound (NMVOC) emissions in China
833 during 1990–2017: drivers, speciation and ozone formation potential, *Atmospheric
834 Chemistry and Physics*, 19, 8897-8913, 10.5194/acp-19-8897-2019, 2019.

835 Li, W., Li, L., Chen, C.-l., Kacarab, M., Peng, W., Price, D., Xu, J., and Cocker, D. R.:
836 Potential of select intermediate-volatility organic compounds and consumer products
837 for secondary organic aerosol and ozone formation under relevant urban conditions,
838 *Atmospheric Environment*, 178, 109-117, 10.1016/j.atmosenv.2017.12.019, 2018.

839 Li, X.-B., Yuan, B., Wang, S., Wang, C., Lan, J., Liu, Z., Song, Y., He, X., Huangfu, Y.,
840 Pei, C., Cheng, P., Yang, S., Qi, J., Wu, C., Huang, S., You, Y., Chang, M., Zheng, H.,
841 Yang, W., Wang, X., and Shao, M.: Variations and sources of volatile organic
842 compounds (VOCs) in urban region: insights from measurements on a tall tower,
843 *Atmospheric Chemistry and Physics*, 22, 10567-10587, 10.5194/acp-22-10567-2022,
844 2022.

845 Li, Y., Pöschl, U., and Shiraiwa, M.: Molecular corridors and parameterizations of
846 volatility in the chemical evolution of organic aerosols, *Atmospheric Chemistry and
847 Physics*, 16, 3327-3344, 10.5194/acp-16-3327-2016, 2016.

848 Liang, Z., Chen, L., Alam, M. S., Zeraati Rezaei, S., Stark, C., Xu, H., and Harrison, R.
849 M.: Comprehensive chemical characterization of lubricating oils used in modern



850 vehicular engines utilizing GC×GC-TOFMS, *Fuel*, 220, 792-799,
851 10.1016/j.fuel.2017.11.142, 2018.

852 Liu, Y., Li, Y., Yuan, Z., Wang, H., Sha, Q., Lou, S., Liu, Y., Hao, Y., Duan, L., Ye, P.,
853 Zheng, J., Yuan, B., and Shao, M.: Identification of two main origins of intermediate-
854 volatility organic compound emissions from vehicles in China through two-phase
855 simultaneous characterization, *Environ Pollut*, 281, 117020,
856 10.1016/j.envpol.2021.117020, 2021.

857 Malherbe, L., and Mandin, C.: VOC emissions during outdoor ship painting and health-
858 risk assessment, *Atmospheric Environment*, 41, 6322-6330,
859 10.1016/j.atmosenv.2007.02.018, 2007.

860 McDonald, B. C., de Gouw, J. A., Gilman, J. B., Jathar, S. H., Akherati, A., Cappa, C.
861 D., Jimenez, J. L., Lee-Taylor, J., Hayes, P. L., McKeen, S. A., Cui, Y. Y., Kim, S.-W.,
862 Gentner, D. R., Isaacman-VanWertz, G., Goldstein, A. H., Harley, R. A., Frost, G. J.,
863 Roberts, J. M., Ryerson, T. B., and Trainer, M.: Volatile chemical products emerging as
864 largest petrochemical source of urban organic emissions, *Science*, 359, 760,
865 10.1126/science.aaq0524, 2018.

866 Mo, Z., Shao, M., and Lu, S.: Compilation of a source profile database for hydrocarbon
867 and OVOC emissions in China, *Atmospheric Environment*, 143, 209-217,
868 10.1016/j.atmosenv.2016.08.025, 2016.

869 Mo, Z., Cui, R., Yuan, B., Cai, H., McDonald, B. C., Li, M., Zheng, J., and Shao, M.:
870 A mass-balance-based emission inventory of non-methane volatile organic compounds
871 (NMVOCs) for solvent use in China, *Atmospheric Chemistry and Physics*, 21, 13655-
872 13666, 10.5194/acp-21-13655-2021, 2021.

873 Na, K., and Pyo Kim, Y.: Chemical mass balance receptor model applied to ambient
874 C₂-C₉ VOC concentration in Seoul, Korea: Effect of chemical reaction losses,
875 *Atmospheric Environment*, 41, 6715-6728,
876 <https://doi.org/10.1016/j.atmosenv.2007.04.054>, 2007.

877 Ou, J., Zheng, J., Li, R., Huang, X., Zhong, Z., Zhong, L., and Lin, H.: Speciated OVOC
878 and VOC emission inventories and their implications for reactivity-based ozone control
879 strategy in the Pearl River Delta region, China, *Sci Total Environ*, 530-531, 393-402,
880 10.1016/j.scitotenv.2015.05.062, 2015.

881 Qin, M., Murphy, B. N., Isaacs, K. K., McDonald, B. C., Lu, Q., McKeen, S. A., Koval,
882 L., Robinson, A. L., Efstathiou, C., Allen, C., and Pye, H. O. T.: Criteria pollutant
883 impacts of volatile chemical products informed by near-field modelling, *Nature*
884 *Sustainability*, 4, 129-137, 10.1038/s41893-020-00614-1, 2021.

885 Rogers, T. M., Grimsrud, E. P., Herndon, S. C., Jayne, J. T., Kolb, C. E., Allwine, E.,
886 Westberg, H., Lamb, B. K., Zavala, M., Molina, L. T., Molina, M. J., and Knighton, W.
887 B.: On-road measurements of volatile organic compounds in the Mexico City
888 metropolitan area using proton transfer reaction mass spectrometry, *International*
889 *Journal of Mass Spectrometry*, 252, 26-37, 10.1016/j.ijms.2006.01.027, 2006.

890 Sasidharan, S., He, Y., Akherati, A., Li, Q., Li, W., Cocker, D., McDonald, B. C.,
891 Coggon, M. M., Seltzer, K. M., Pye, H. O. T., Pierce, J. R., and Jathar, S. H.: Secondary
892 Organic Aerosol Formation from Volatile Chemical Product Emissions: Model



893 Parameters and Contributions to Anthropogenic Aerosol, *Environmental Science &*
894 *Technology*, 57, 11891-11902, 10.1021/acs.est.3c00683, 2023.

895 Sekimoto, K., Li, S.-M., Yuan, B., Koss, A., Coggon, M., Warneke, C., and de Gouw,
896 J.: Calculation of the sensitivity of proton-transfer-reaction mass spectrometry (PTR-
897 MS) for organic trace gases using molecular properties, *International Journal of Mass*
898 *Spectrometry*, 421, 71-94, 10.1016/j.ijms.2017.04.006, 2017.

899 Seltzer, K. M., Pennington, E., Rao, V., Murphy, B. N., Strum, M., Isaacs, K. K., and
900 Pye, H. O. T.: Reactive organic carbon emissions from volatile chemical products,
901 *Atmos Chem Phys*, 21, 5079-5100, 10.5194/acp-21-5079-2021, 2021.

902 Seltzer, K. M., Murphy, B. N., Pennington, E. A., Allen, C., Talgo, K., and Pye, H. O.
903 T.: Volatile Chemical Product Enhancements to Criteria Pollutants in the United States,
904 *Environ Sci Technol*, 56, 6905-6913, 10.1021/acs.est.1c04298, 2022.

905 Sha, Q., Zhu, M., Huang, H., Wang, Y., Huang, Z., Zhang, X., Tang, M., Lu, M., Chen,
906 C., Shi, B., Chen, Z., Wu, L., Zhong, Z., Li, C., Xu, Y., Yu, F., Jia, G., Liao, S., Cui, X.,
907 Liu, J., and Zheng, J.: A newly integrated dataset of volatile organic compounds (VOCs)
908 source profiles and implications for the future development of VOCs profiles in China,
909 *Sci Total Environ*, 793, 148348, 10.1016/j.scitotenv.2021.148348, 2021.

910 Shi, Y., Xi, Z., Lv, D., Simayi, M., Liang, Y., Ren, J., and Xie, S.: Sector-based volatile
911 organic compound emission characteristics and reduction perspectives for coating
912 materials manufacturing in China, *Journal of Cleaner Production*, 394,
913 10.1016/j.jclepro.2023.136407, 2023.

914 Song, X., Yuan, B., Wang, S., He, X., Li, X., Peng, Y., Chen, Y., Qi, J., Cai, J., Huang,
915 s., Hu, D., Wei, W., Liu, K., and Shao, M.: Compositional Characteristics of Volatile
916 Organic Compounds in Typical Industrial Areas of the Pearl River Delta: Importance
917 of Oxygenated Volatile Organic Compounds (in Chinese), *Environmental Science*,
918 10.13227/j.hjxk.202204104, 2023.

919 Stark, H., Yatavelli, R. L. N., Thompson, S. L., Kimmel, J. R., Cubison, M. J., Chhabra,
920 P. S., Canagaratna, M. R., Jayne, J. T., Worsnop, D. R., and Jimenez, J. L.: Methods to
921 extract molecular and bulk chemical information from series of complex mass spectra
922 with limited mass resolution, *International Journal of Mass Spectrometry*, 389, 26-38,
923 10.1016/j.ijms.2015.08.011, 2015.

924 Stockwell, C. E., Coggon, M. M., Gkatzelis, G. I., Ortega, J., McDonald, B. C., Peischl,
925 J., Aikin, K., Gilman, J. B., Trainer, M., and Warneke, C.: Volatile organic compound
926 emissions from solvent- and water-borne coatings – compositional differences and
927 tracer compound identifications, *Atmospheric Chemistry and Physics*, 21, 6005-6022,
928 10.5194/acp-21-6005-2021, 2021.

929 Sulzer, P., Hartungen, E., Hanel, G., Feil, S., Winkler, K., Mutschlechner, P., Haidacher,
930 S., Schottkowsky, R., Gansch, D., Seehauser, H., Striednig, M., Jürschik, S., Breiev, K.,
931 Lanza, M., Herbig, J., Märk, L., Märk, T. D., and Jordan, A.: A Proton Transfer
932 Reaction-Quadrupole interface Time-Of-Flight Mass Spectrometer (PTR-QiTOF):
933 High speed due to extreme sensitivity, *International Journal of Mass Spectrometry*, 368,
934 1-5, 10.1016/j.ijms.2014.05.004, 2014.



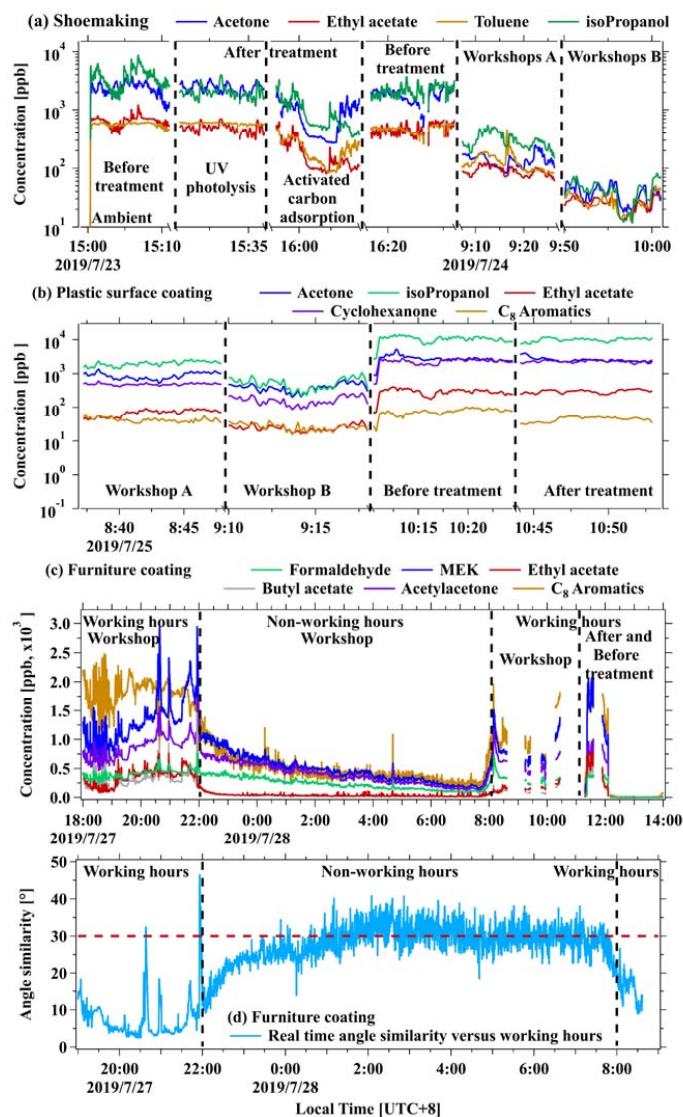
- 935 Sun, W., Shao, M., Granier, C., Liu, Y., Ye, C. S., and Zheng, J. Y.: Long-Term Trends
936 of Anthropogenic SO₂, NO_x, CO, and NMVOCs Emissions in China, *Earth's Future*, 6,
937 1112-1133, 10.1029/2018ef000822, 2018.
- 938 Ulbrich, I. M., Canagaratna, M. R., Zhang, Q., Worsnop, D. R., and Jimenez, J. L.:
939 Interpretation of organic components from Positive Matrix Factorization of aerosol
940 mass spectrometric data, *Atmos. Chem. Phys.*, 9, 2891-2918, 10.5194/acp-9-2891-2009,
941 2009.
- 942 Wang, C., Yuan, B., Wu, C., Wang, S., Qi, J., Wang, B., Wang, Z., Hu, W., Chen, W.,
943 Ye, C., Wang, W., Sun, Y., Wang, C., Huang, S., Song, W., Wang, X., Yang, S., Zhang,
944 S., Xu, W., Ma, N., Zhang, Z., Jiang, B., Su, H., Cheng, Y., Wang, X., and Shao, M.:
945 Measurements of higher alkanes using NO⁺ chemical ionization in PTR-ToF-MS:
946 important contributions of higher alkanes to secondary organic aerosols in China,
947 *Atmospheric Chemistry and Physics*, 20, 14123-14138, 10.5194/acp-20-14123-2020,
948 2020.
- 949 Wang, H., Qiao, Y., Chen, C., Lu, J., Dai, H., Qiao, L., Lou, S., Huang, C., Li, L., Jing,
950 S., and Wu, J.: Source Profiles and Chemical Reactivity of Volatile Organic Compounds
951 from Solvent Use in Shanghai, China, *Aerosol and Air Quality Research*, 14, 301-310,
952 10.4209/aaqr.2013.03.0064, 2014.
- 953 Wang, R., Zhang, C., Ding, H., LV, S., Ding, Y., Wang, H., and Wang, B.: Emission
954 characteristics of volatile organic compounds (VOCs) from the production processes of
955 plastic parts in electronic manufacturing industry (in Chinese), *Acta Scientiae*
956 *Circumstantiae*, 39, 4-12, 10.13671/j.hjkxxb.2018.0243, 2019.
- 957 Wang, S., Yuan, B., Wu, C., Wang, C., Li, T., He, X., Huangfu, Y., Qi, J., Li, X. B., Sha,
958 Q., Zhu, M., Lou, S., Wang, H., Karl, T., Graus, M., Yuan, Z., and Shao, M.: Oxygenated
959 volatile organic compounds (VOCs) as significant but varied contributors to VOC
960 emissions from vehicles, *Atmos. Chem. Phys.*, 22, 9703-9720, 10.5194/acp-22-9703-
961 2022, 2022.
- 962 Wei, W., Wang, S., Hao, J., and Cheng, S.: Projection of anthropogenic volatile organic
963 compounds (VOCs) emissions in China for the period 2010–2020, *Atmospheric*
964 *Environment*, 45, 6863-6871, <https://doi.org/10.1016/j.atmosenv.2011.01.013>, 2011.
- 965 Wu, C., Wang, C., Wang, S., Wang, W., Yuan, B., Qi, J., Wang, B., Wang, H., Wang, C.,
966 Song, W., Wang, X., Hu, W., Lou, S., Ye, C., Peng, Y., Wang, Z., Huangfu, Y., Xie, Y.,
967 Zhu, M., Zheng, J., Wang, X., Jiang, B., Zhang, Z., and Shao, M.: Measurement report:
968 Important contributions of oxygenated compounds to emissions and chemistry of
969 volatile organic compounds in urban air, *Atmospheric Chemistry and Physics*, 20,
970 14769-14785, 10.5194/acp-20-14769-2020, 2020a.
- 971 Wu, J., Gao, S., Chen, X., Yang, Y., Fu, Q.-y., Che, X., and Jiao, Z.: Source Profiles and
972 Impact of Volatile Organic Compounds in the Coating Manufacturing Industry (in
973 Chinese), *Environmental Science*, 41, 1582-1588, 10.13227/j.hjkx.201908203, 2020b.
- 974 Yang, G., Huo, J., Wang, L., Wang, Y., Wu, S., Yao, L., Fu, Q., and Wang, L.: Total OH
975 Reactivity Measurements in a Suburban Site of Shanghai, *Journal of Geophysical*
976 *Research: Atmospheres*, 127, 10.1029/2021jd035981, 2022.



- 977 Yang, Y., Shao, M., Wang, X., Nölscher, A. C., Kessel, S., Guenther, A., and Williams,
978 J.: Towards a quantitative understanding of total OH reactivity: A review, *Atmospheric*
979 *Environment*, 134, 147-161, <https://doi.org/10.1016/j.atmosenv.2016.03.010>, 2016.
- 980 Yuan, B., Shao, M., Lu, S., and Wang, B.: Source profiles of volatile organic compounds
981 associated with solvent use in Beijing, China, *Atmospheric Environment*, 44, 1919-
982 1926, [10.1016/j.atmosenv.2010.02.014](https://doi.org/10.1016/j.atmosenv.2010.02.014), 2010.
- 983 Yuan, B., Koss, A. R., Warneke, C., Coggon, M., Sekimoto, K., and de Gouw, J. A.:
984 Proton-Transfer-Reaction Mass Spectrometry: Applications in Atmospheric Sciences,
985 *Chemical Reviews*, 117, 13187-13229, [10.1021/acs.chemrev.7b00325](https://doi.org/10.1021/acs.chemrev.7b00325), 2017.
- 986 Zhao, J., Yao, X., Sun, M., Xu, Y., Wang, S., Cao, D., and Liu, J.: Emission
987 characteristics of volatile organic compounds from typical solvent use industries in
988 Tianjin (in Chinese), *Environmental Pollution & Control*, 43, 539-545,
989 [10.15985/j.cnki.1001-3865.2021.05.002](https://doi.org/10.15985/j.cnki.1001-3865.2021.05.002), 2021.
- 990 Zhao, R., Huang, L., Zhang, J., and Ouyang, F.: Emissions characteristics of volatile
991 organic compounds (VOCs) from typical industries of solvent use in Chengdu City (in
992 Chinese), *Acta Scientiae Circumstantiae*, 38, 1147-1154, [10.13671/j.hjkxxb.2017.0362](https://doi.org/10.13671/j.hjkxxb.2017.0362),
993 2018a.
- 994 Zhao, Y., Hennigan, C. J., May, A. A., Tkacik, D. S., de Gouw, J. A., Gilman, J. B.,
995 Kuster, W. C., Borbon, A., and Robinson, A. L.: Intermediate-volatility organic
996 compounds: a large source of secondary organic aerosol, *Environ Sci Technol*, 48,
997 13743-13750, [10.1021/es5035188](https://doi.org/10.1021/es5035188), 2014.
- 998 Zhao, Y., Nguyen, N. T., Presto, A. A., Hennigan, C. J., May, A. A., and Robinson, A.
999 L.: Intermediate Volatility Organic Compound Emissions from On-Road Gasoline
1000 Vehicles and Small Off-Road Gasoline Engines, *Environmental Science & Technology*,
1001 50, 4554-4563, [10.1021/acs.est.5b06247](https://doi.org/10.1021/acs.est.5b06247), 2016.
- 1002 Zhao, Y., Lambe, A. T., Saleh, R., Saliba, G., and Robinson, A. L.: Secondary Organic
1003 Aerosol Production from Gasoline Vehicle Exhaust: Effects of Engine Technology,
1004 Cold Start, and Emission Certification Standard, *Environ Sci Technol*, 52, 1253-1261,
1005 [10.1021/acs.est.7b05045](https://doi.org/10.1021/acs.est.7b05045), 2018b.
- 1006 Zheng, J., Yu, Y., Mo, Z., Zhang, Z., Wang, X., Yin, S., Peng, K., Yang, Y., Feng, X.,
1007 and Cai, H.: Industrial sector-based volatile organic compound (VOC) source profiles
1008 measured in manufacturing facilities in the Pearl River Delta, China, *Sci Total Environ*,
1009 456-457, 127-136, [10.1016/j.scitotenv.2013.03.055](https://doi.org/10.1016/j.scitotenv.2013.03.055), 2013.
- 1010 Zhong, Z., Sha, Q., Zheng, J., Yuan, Z., Gao, Z., Ou, J., Zheng, Z., Li, C., and Huang,
1011 Z.: Sector-based VOCs emission factors and source profiles for the surface coating
1012 industry in the Pearl River Delta region of China, *Sci Total Environ*, 583, 19-28,
1013 [10.1016/j.scitotenv.2016.12.172](https://doi.org/10.1016/j.scitotenv.2016.12.172), 2017.
- 1014 Zhong, Z., Zheng, J., Zhu, M., Huang, Z., Zhang, Z., Jia, G., Wang, X., Bian, Y., Wang,
1015 Y., and Li, N.: Recent developments of anthropogenic air pollutant emission inventories
1016 in Guangdong province, China, *Sci Total Environ*, 627, 1080-1092,
1017 [10.1016/j.scitotenv.2018.01.268](https://doi.org/10.1016/j.scitotenv.2018.01.268), 2018.
- 1018 Zhou, Z., Deng, Y., Zhou, X., Wu, K., TAN, Q., Yin, D., Song, D., Chen, Q., and Zeng,
1019 W.: Source Profiles of Industrial Emission-Based VOCs in Chengdu (in Chinese),
1020 *Environmental Science*, 41, 3042-3055, [10.13227/j.hjkx.201912203](https://doi.org/10.13227/j.hjkx.201912203), 2020a.



1021 Zhou, Z., Tan, Q., Deng, Y., Song, D., Wu, K., Zhou, X., Huang, F., Zeng, W., and Lu,
1022 C.: Compilation of emission inventory and source profile database for volatile organic
1023 compounds: A case study for Sichuan, China, Atmospheric Pollution Research, 11, 105-
1024 116, <https://doi.org/10.1016/j.apr.2019.09.020>, 2020b.
1025 Zhu, W., Guo, S., Zhang, Z., Wang, H., Yu, Y., Chen, Z., Shen, R., Tan, R., Song, K.,
1026 Liu, K., Tang, R., Liu, Y., Lou, S., Li, Y., Zhang, W., Zhang, Z., Shuai, S., Xu, H., Li,
1027 S., Chen, Y., Hu, M., Canonaco, F., and Prévôt, A. S. H.: Mass spectral characterization
1028 of secondary organic aerosol from urban cooking and vehicular sources, Atmospheric
1029 Chemistry and Physics, 21, 15065-15079, 10.5194/acp-21-15065-2021, 2021.
1030



1031

1032

1033

1034

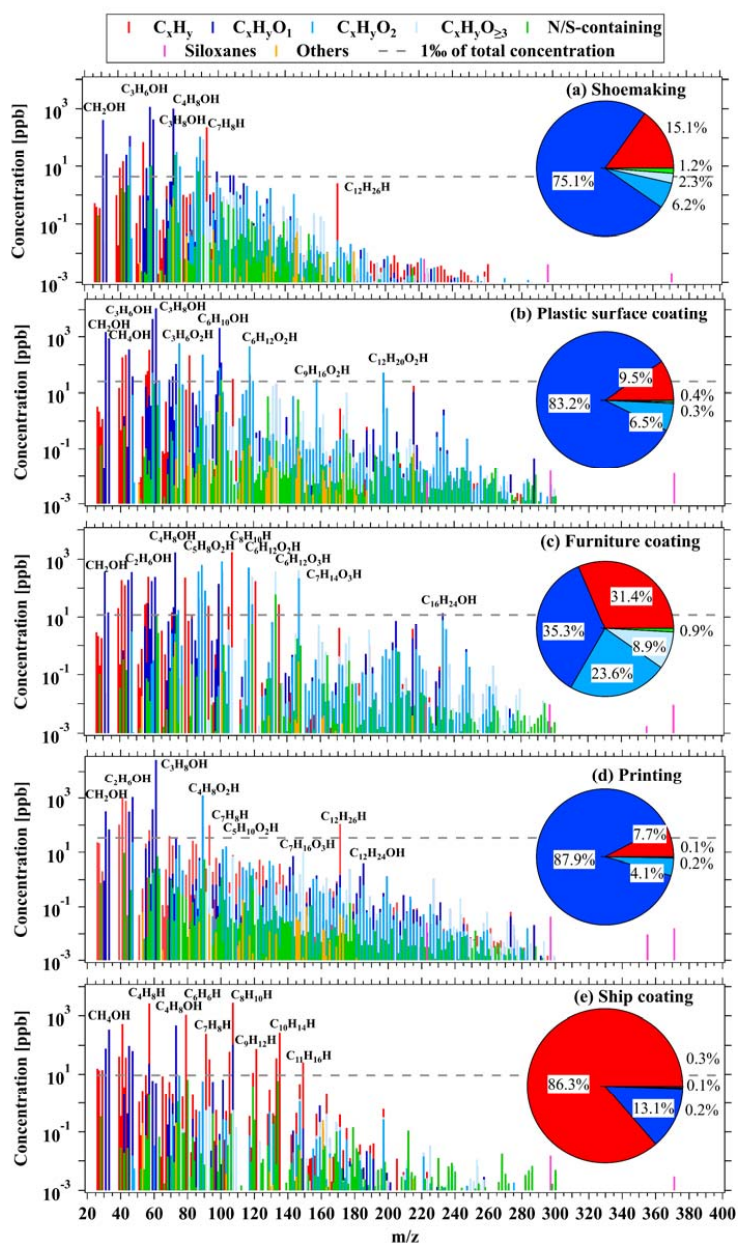
1035

1036

1037

1038

Figure 1. Real-time concentrations of representative ROGs from workshops, before and after the ROG treatment devices in (a) shoe making industry and (b) plastic surface coating industry, and (c) during working hours or non-working hours in the furniture coating industry. (d) The θ angles of mass spectra among real-time concentrations versus average concentration during working time (19:00-22:00) in the furniture coating industry.



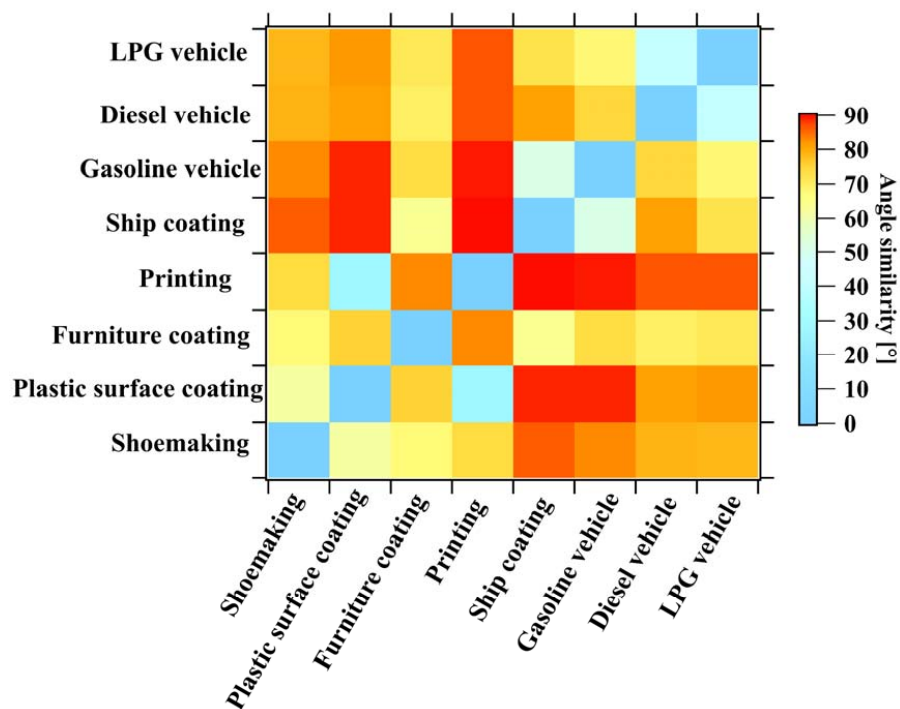
1039

1040 **Figure 2.** Average concentrations and fractions of ROGs measured by PTR-ToF-MS

1041 from stack emissions of (a) shoemaking, (b) plastic surface coating, (c) furniture coating,

1042 (d) printing, and (e) ship coating industries.

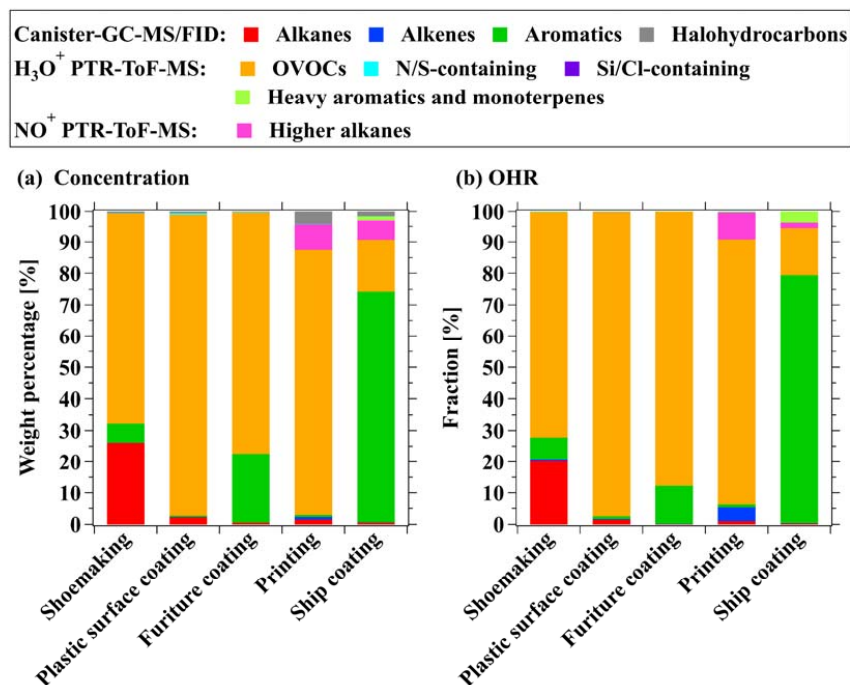
1043



1044

1045 **Figure 3.** The θ angles ($^{\circ}$) among the mass spectra of industrial VCP sources in this
1046 study and vehicular emissions from previous study (Wang et al., 2022).

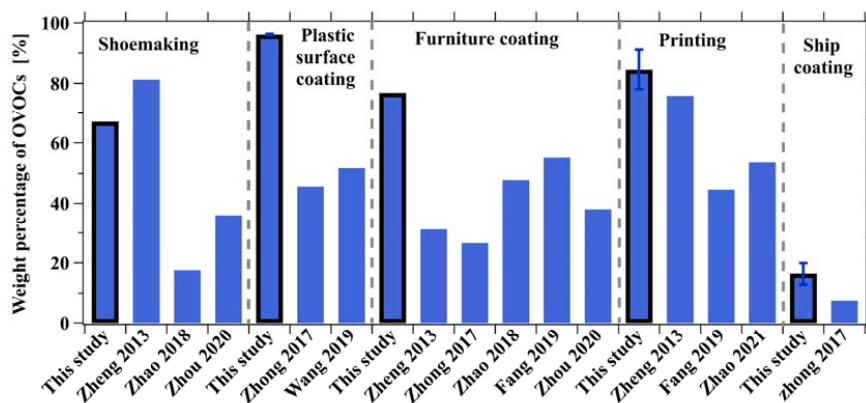
1047



1048

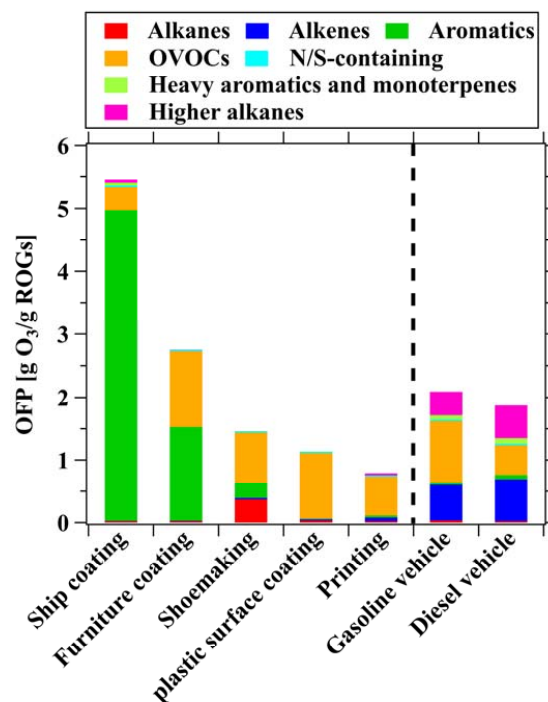
1049 **Figure 4.** Fractions of (a) concentrations and (b) OHR for ROG components to total
 1050 ROGs from stack emissions from shoemaking, plastic surface coating, furniture coating,
 1051 printing, and ship coating industries.

1052



1053

1054 **Figure 5.** Comparison of OVOC fractions determined from stack emission of industrial
1055 VCP sources in this study and those in previous studies. Error bars represent the
1056 standard deviations of the weight percentage of OVOCs.
1057

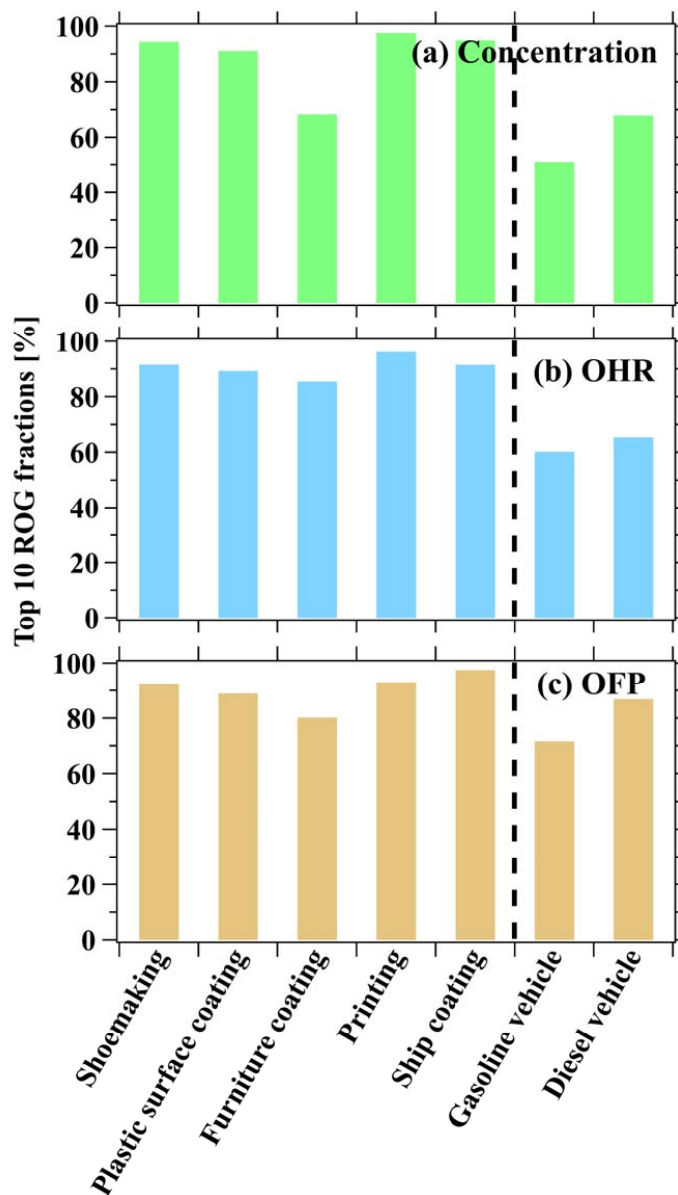


1058

1059 **Figure 6.** Comparison of OFP among various industrial VCP sources in this study and

1060 vehicular emissions from previous study (Wang et al., 2022).

1061



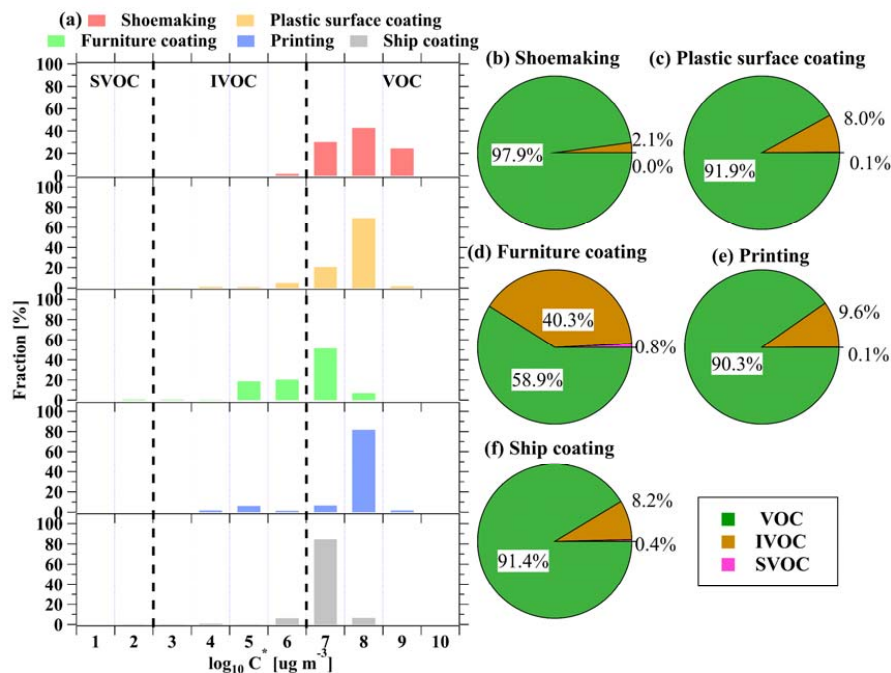
1062

1063 **Figure 7.** Accumulated fractions of the top ten species in total (a) ROG emissions, (b)

1064 OHR, and (c) OFP from industrial VCP sources in this study and vehicular emissions

1065 from previous study (Wang et al., 2022).

1066

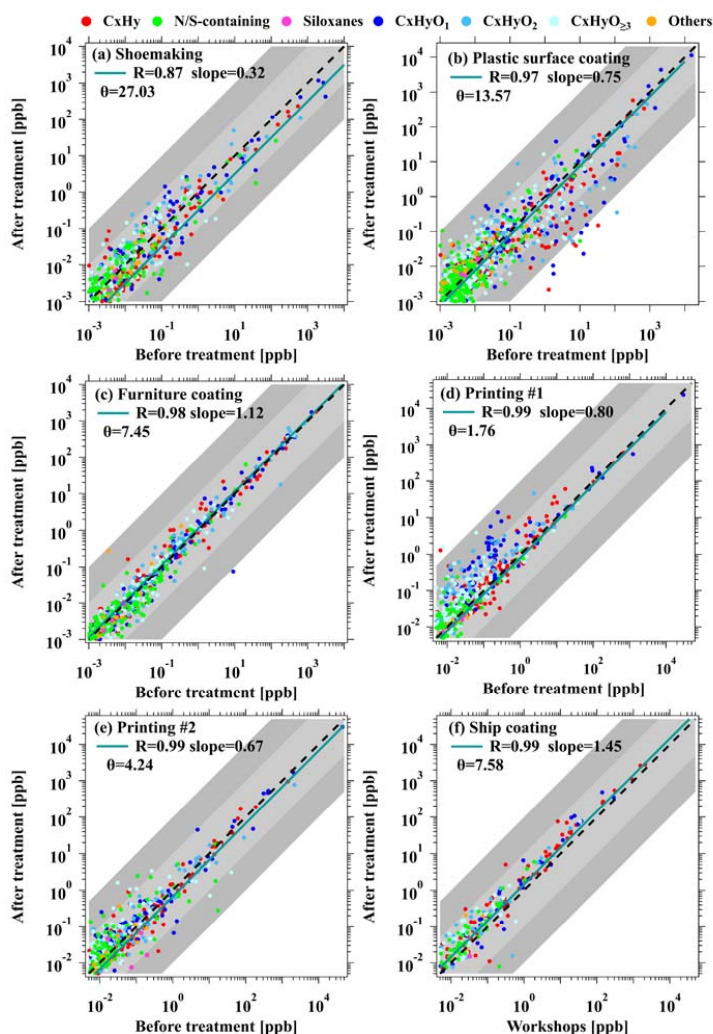


1067

1068 **Figure 8.** (a) Volatility-binned fractions from stack emissions of various industrial VCP
 1069 sources, and volatility-binned fractions in different ROG categories from stack
 1070 emissions of (b) shoemaking, (c) plastic surface coating, (d) furniture coating, (e)
 1071 printing, and (f) ship coating industries.

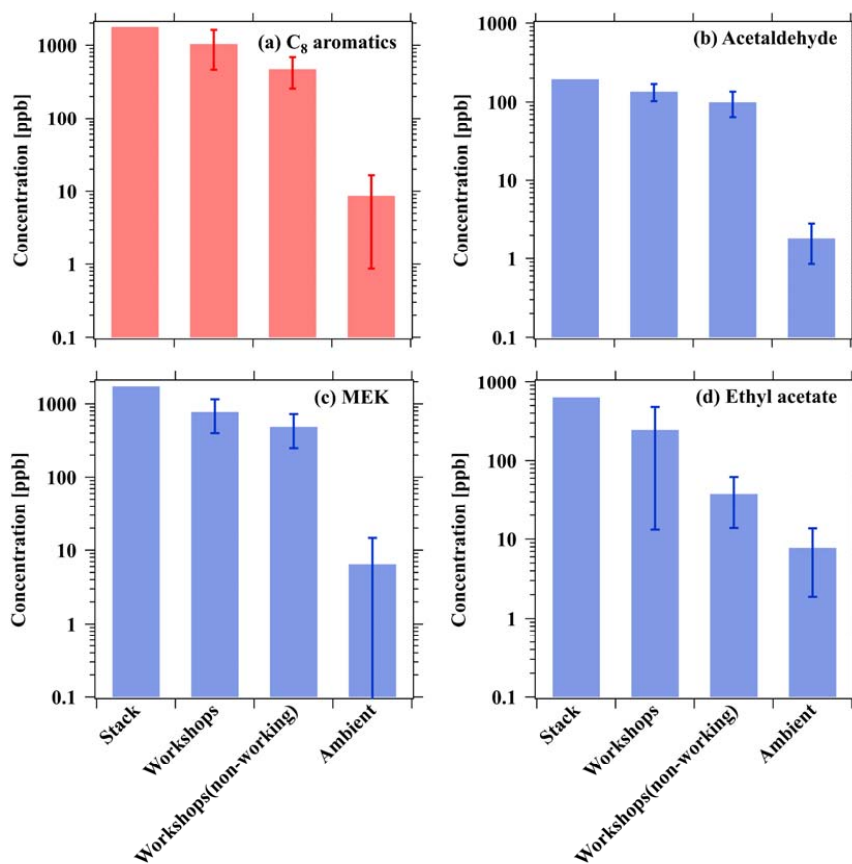
1072

1073



1074
1075 **Figure 9.** Scatterplots of ROG concentrations between before and after treatment with
1076 activated carbon adsorption + UV photolysis for (a) shoemaking, (b) plastics surface
1077 coating, (c) furniture coating, and (d) printing industries. Scatterplots of ROG
1078 concentrations between before and after treatment with catalytic combustion for (e) the
1079 printing industry, and ROG concentrations between workshops and after treatment with
1080 catalytic combustion (f) the ship coating industry. The green lines are the fitted results
1081 for all data points. The black dashed lines represent 1:1 ratio, and the shaded areas
1082 represent ratios of a factor of 10 and 100.

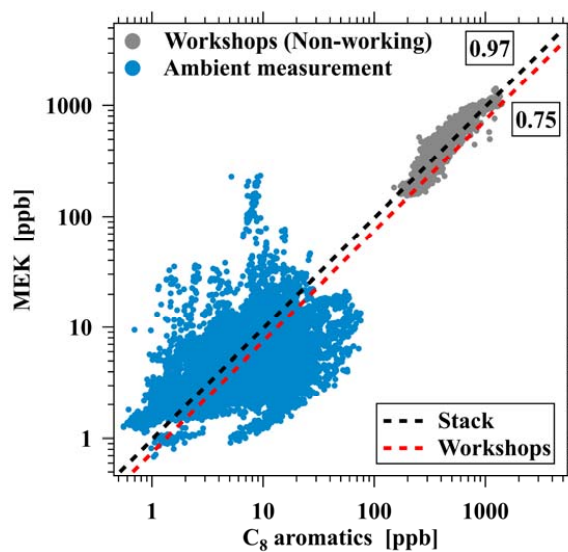
1083



1084

1085 **Figure 10.** Average concentrations of (a) C₈ aromatics, (b) acetaldehyde, (c) MEK, and
1086 (d) ethyl acetate emission from the stack, workshops during working and non-working
1087 hours in the furniture coating industry and ambient measurement near the industry,
1088 respectively. Error bars represent the standard deviations of the concentration.

1089



1090

1091 **Figure 11.** Scatterplot of MEK versus C₈ aromatics at workshops during non-working
1092 hours in the furniture coating industry and ambient measurement near the industry. The
1093 black and red dashed line represent ratios of ROG pairs for stack and workshops
1094 emission in furniture coating industry.

1095